

AD-757 516

EFFECTS OF STRAIN AMPLITUDE ON THE SHEAR  
MODULUS OF SOILS

Bobby O. Hardin

Kentucky University

Prepared for:

Air Force Weapons Laboratory

March 1973

DISTRIBUTED BY:

**NTIS**

National Technical Information Service  
U. S. DEPARTMENT OF COMMERCE  
5285 Port Royal Road, Springfield Va. 22151

AD757516

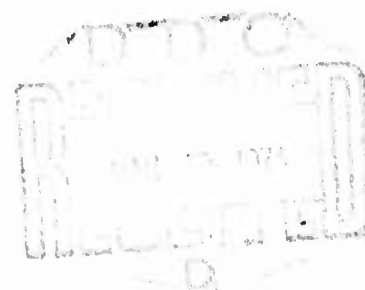


# EFFECTS OF STRAIN AMPLITUDE ON THE SHEAR MODULUS OF SOILS

Bobby O. Hardin  
University of Kentucky

TECHNICAL REPORT NO. AFWL-TR-72-201

March 1973



**AIR FORCE WEAPONS LABORATORY**  
Air Force Systems Command  
Kirtland Air Force Base  
New Mexico

Reproduced by  
**NATIONAL TECHNICAL  
INFORMATION SERVICE**  
U S Department of Commerce  
Springfield VA 22151

Approved for public release; distribution unlimited.



AFWL-TR-72-201

EFFECTS OF STRAIN AMPLITUDE ON THE  
SHEAR MODULUS OF SOILS

Bobby O. Hardin  
University of Kentucky

TECHNICAL REPORT NO. AFWL-TR-72-201

Approved for public release; distribution unlimited.

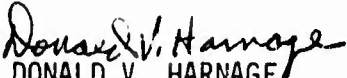
FOREWORD

This report was prepared by the University of Kentucky, Lexington, Kentucky, under Contract F29601-72-C-0027. The research was performed under Program Element 63723F, Project 683M, Task 4A06.

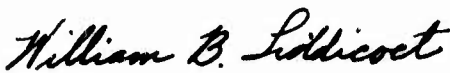
Inclusive dates of research were 10 October 1972 through 2 November 1972. The report was submitted 9 January 1973 by the Air Force Weapons Laboratory Project Officer, Major Donald V. Harnage (DEZ).

The Contractor's report number is UKY TR63-72-CE23.

This technical report has been reviewed and is approved.

  
DONALD V. HARNAGE  
Major, USAF  
Project Officer

  
OREN G. STROM  
Lt Colonel, USAF  
Chief, Aerospace Facility Branch

  
WILLIAM B. LIDDICOET  
Colonel, USAF  
Chief, Civil Engineering Research  
Division

UNCLASSIFIED

Security Classification

DOCUMENT CONTROL DATA - R & D

(Security classification of title, body of abstract and indexing annotation must be entered when the overall report is classified)

1. ORIGINATING ACTIVITY (Corporate author) University of Kentucky, Department of Civil Engineering Lexington, Kentucky 40506		2a. REPORT SECURITY CLASSIFICATION UNCLASSIFIED	
		2b. GROUP	
3. REPORT TITLE EFFECTS OF STRAIN AMPLITUDE ON THE SHEAR MODULUS OF SOILS			
4. DESCRIPTIVE NOTES (Type of report and inclusive dates) 1 October 1971-1 November 1972			
5. AUTHOR(S) (First name, middle initial, last name) Bobby O. Hardin			
6. REPORT DATE March 1973		7a. TOTAL NO. OF PAGES 74	7b. NO. OF REFS 2
8a. CONTRACT OR GRANT NO. F29601-72-C-0027	b. PROJECT NO. 683M	9a. ORIGINATOR'S REPORT NUMBER(S) AFWL-TR-72-201	
c. Task No. 4A06	d.	9b. OTHER REPORT NO(S) (Any other numbers that may be assigned this report) Contractor's report number: UKY TR63-72-CE23	
10. DISTRIBUTION STATEMENT Approved for public release; distribution unlimited.			
11. SUPPLEMENTARY NOTES		12. SPONSORING MILITARY ACTIVITY AFWL (DEZ) Kirtland AFB, NM 87117	
13. ABSTRACT (Distribution Limitation Statement A) One hundred twenty-three simple shear tests of 24 different soils were conducted. Most were constant-amplitude repeated load tests. A few of the tests involved mixed amplitudes of loading with rest periods between loads. Based on the results, a practical procedure for reducing the shear modulus of soils with increasing strain amplitude was developed. It was shown that for a wide variety of soil types and conditions the procedure gives reasonably accurate results compared to values measured in the laboratory. The study of mixed amplitudes and rest periods indicated that the procedure can be applied to mixed traffic conditions.			

14. KEY WORDS	LINK A		LINK B		LINK C	
	ROLE	WT	ROLE	WT	ROLE	WT
Civil engineering Airfield pavements Rigid pavements Flexible pavements						

## ABSTRACT

(Distribution Limitation Statement A)

One hundred twenty-three simple shear tests of 24 different soils were conducted. Most were constant-amplitude repeated load tests. A few of the tests involved mixed amplitudes of loading with rest periods between loads. Based on the results, a practical procedure for reducing the shear modulus of soils with increasing strain amplitude was developed. It was shown that for a wide variety of soil types and conditions the procedure gives reasonably accurate results compared to values measured in the laboratory. The study of mixed amplitudes and rest periods indicated that the procedure can be applied to mixed traffic conditions.

## TABLE OF CONTENTS

<u>Section</u>	<u>Page</u>
I INTRODUCTION. . . . .	1
1. Pavement Evaluation . . . . .	1
2. Review of Previous Report . . . . .	2
3. Current Testing Program . . . . .	2
II A PRACTICAL PROCEDURE FOR REDUCTION OF SHEAR MODULUS WITH INCREASING STRAIN LEVEL . . . . .	4
1. Objective . . . . .	4
2. Definitions . . . . .	4
3. Determination of the Reference Strain . . . . .	6
4. Determination of the Shear Modulus . . . . .	9
5. Examples of Use of the Procedure . . . . .	18
III COMPARISON OF VALUES FROM THE PRACTICAL PROCEDURE TO EXPERIMENTAL DATA. . . . .	21
1. Soils Tested . . . . .	21
2. Values of R for Determination of Reference Strain . . . . .	21
3. Comparison of Shear Modulus Values . . . . .	34
IV MIXED LOADING AMPLITUDES AND REST PERIODS . . . . .	46
1. Objective . . . . .	46
2. Loading Programs and Recorded Stress-Strain Relations . . . . .	46
3. Effect on the Shear Modulus . . . . .	53
V CONCLUSIONS . . . . .	56
Appendix I . . . . .	59
Appendix II . . . . .	61

## LIST OF FIGURES

<u>Figure</u>		<u>Page</u>
1	Schematic simple shear stress-strain relation.	5
2	Value of $C_1$ versus void ratio for sands with less than 15 percent fines.	8
3	Value of $C_1$ versus plasticity index, percent saturation, and void ratio for cohesive soils with more than 15 percent fines.	10
4	Reference strain versus value of $C_1$ and maximum shear modulus.	11
5	Hyperbolic strain versus normalized strain for various numbers of cycles and rates of loading.	13
6	Hyperbolic strain versus normalized strain for various numbers of cycles and percents saturation, fast rate of loading, $T = 0.01$ , nonplastic soils with fines and low plasticity soils.	14
7	Hyperbolic strain versus normalized strain for various numbers of cycles and percents saturation, slow rate of loading, $T = 10$ , nonplastic soils with fines and low plasticity soils.	15
8	Hyperbolic strain versus normalized strain for numbers of cycles, percents saturation, and rates of loading, high plasticity soils.	16
9	Normalized shear modulus versus hyperbolic strain.	17
10	Particle size distribution curves for nonplastic soils.	27
11	Particle size distribution curves for low plasticity soils.	28
12	Particle size distribution curves for high plasticity soils.	29
13	Comparison of the variation of experimental and calculated values of $R$ with percent saturation,	

<u>Figure</u>		<u>Page</u>
	Air Force Silty Sand, Air Force Silty Clay, Vicksburg Loess, Vanceburg, Allen, Kentucky 55, Longhorn, and West Virginia Shale.	30
14	Comparison of the variation of experimental and calculated values of R with percent saturation, Six Kirtland Soils, Virginia Clay, Dover, Prestonsburg Sand, Ellsworth, Louisiana Clay, San Francisco Clay, Cheeks, and Nevada Clay.	31
15	Variation of normalized shear modulus with normalized strain as given by the practical procedure for various values of a.	35
16	Comparison of measured and calculated values of shear modulus, first cycle, WES Sand, St. John's Sand, and Air Force Silty Sand.	36
17	Comparison of measured and calculated values of shear modulus, first cycle, Air Force Silty Clay, Vicksburg Loess, and Vanceburg.	37
18	Comparison of measured and calculated values of shear modulus, first cycle, Allen, Kentucky 55, and Longhorn.	38
19	Comparison of measured and calculated values of shear modulus, first cycle, West Virginia Shale, Virginia Clay, and Dover.	39
20	Comparison of measured and calculated values of shear modulus, first cycle, Prestonsburg Sand, Kirtland #10-36, and Louisiana Clay.	40
21	Comparison of measured and calculated values of shear modulus, first cycle, San Francisco Clay, Ellsworth, and Cheeks.	41
22	Comparison of measured and calculated values of shear modulus, first cycle, Nevada Clay.	42
23	Comparison of measured and calculated values of shear modulus, 10th cycle.	44

<u>Figure</u>		<u>Page</u>
24	Comparison of measured and calculated values of shear modulus, 100th cycle.	45
25	Loading Programs.	47
26	Recorded stress-strain relation, increasing load sequence, silty clay.	49
27	Recorded stress-strain relation, increasing load sequence, silty clay.	50
28	Recorded stress-strain relation, increasing load sequence, Vicksburg Loess.	51
29	Recorded stress-strain relation, decreasing load sequence	52
30	Normalized shear modulus versus normalized strain for silty clay, mixed amplitudes and rest periods.	54
31	Normalized shear modulus versus normalized strain for silty sand, mixed amplitudes and rest periods.	55
32	Typical Recorded Stress-Strain Relations.	62

## LIST OF TABLES

<u>Table</u>		<u>Page</u>
1	Data for Simple Shear Tests of Clean Sands and other Sands with High Permeability.	22
2	Data for Simple Shear Tests of Nonplastic Silty Sands.	22
3	Data for Simple Shear Tests of Low Plasticity Soils.	24
4	Data for Simple Shear Tests of High Plasticity Soils.	26
5	Values of R for Sands with Less than 15 Percent Fines.	33

## ABBREVIATIONS AND SYMBOLS

a	= parameter in modified hyperbolic stress-strain relation
C <sub>1</sub>	= parameter defined by equations 4 and 5
e	= void ratio
e <sub>xp</sub>	= base of natural logarithms
F	= function of void ratio defined by equation 2
G	= shear modulus
G <sub>max</sub>	= maximum shear modulus
N	= number of cycles
PI	= plasticity index
R	= parameter relating G <sub>max</sub> and τ <sub>max</sub>
S	= percent saturation
T	= time in minutes to reach a normalized strain equal to one
γ	= shear strain
γ <sub>h</sub>	= hyperbolic strain
γ <sub>r</sub>	= reference strain
σ <sub>cham</sub>	= chamber pressure
σ <sub>o</sub>	= effective mean principal stress
φ	= effective angle of shearing resistance
τ <sub>max</sub>	= maximum shear stress

## SECTION I

### INTRODUCTION

#### 1. Pavement Evaluation

This document reports research that is part of a larger Air Force Weapons Laboratory project to develop a pavement evaluation procedure. The following steps are involved in the pavement evaluation procedure, which for the present uses linear elastic analysis for determination of the stresses and strains in the pavement structure.

The first step is to measure the shear modulus for different layers of the pavement structure in-situ, using a nondestructive vibration testing method. The shear modulus thus measured will be for very small strain amplitudes, on the order of  $10^{-5}$  in/in or less. Because the stress-strain relations for paving materials are nonlinear, the secant shear modulus for larger strain amplitudes produced by an aircraft loading will be smaller than the modulus measured by the nondestructive testing method.

The second step is to make the proper reduction in the measured shear modulus to correspond to the strain produced by an aircraft loading.

The third step is to use this shear modulus in a finite-element analysis for stresses and strains in pavement structure under load.

The fourth and final step is to assess the amount of damage or pavement distress that will be produced by the loading.

This report presents a procedure for the second step, the reduction of shear modulus with increasing strain level.

2. Review of Previous Report

The first phase in developing a procedure for the reduction of shear modulus with increasing strain level was to design and construct testing equipment capable of accurate measurement of the shear stress-strain relation for soils, over a wide range of strain levels. The range was from about  $10^{-5}$  in/in to failure, i.e., after a given number of constant-amplitude cyclic loads each sample was loaded to failure. Also, a series of tests with two soils, a silty sand and a silty clay, were conducted to assess the relative effects of various parameters, such as density, percent saturation and confining stress, on the shear stress-strain relation for cyclic loading. Reference 1 reports on this phase of the research, and the testing equipment, its capabilities, and the testing procedure developed are described in detail. Examples of recorded stress-strain curves are given, and the methods of analysis of the data are discussed. The same equipment, procedures, and most of the methods of analysis were used for the current testing program. They will not be described in detail herein, since the information is available in reference 1. However, a brief description of methods and procedures is given in Appendix II. Some of the definitions presented in Section II are amplified in reference 1.

3. Current Testing Program

The objective of the current testing program was to determine whether

- 
1. Hardin, Bobby O., Characterization and Use of Shear Stress-Strain Relations for Airfield Subgrade and Base Course Materials, Technical Report No. AFWL-TR-71-60, Air Force Weapons Laboratory, Kirtland AFB, NM, July 1971.

or not the characterization of the shear stress-strain relation presented in reference 1 is applicable to a wide variety of soils. A total of 80 specimens of 20 different soils were tested with differing parameters, such as soil type, strain amplitude, density, and percent saturation. Including Phase I, a total of 129 tests on 24 different soils have been conducted and analyzed. Data for only six tests appeared to be faulty (i. e., an error in conducting the test) and were thrown out. The relationships presented here are based on 123 tests of 24 different soils.

A procedure for reducing the shear modulus with increasing strain level, recommended for use in the Air Force pavement evaluation technique, is presented in Section II. In Section III values of the shear modulus determined by this procedure are compared to the experimental data in order to verify the procedure and to show the probable magnitude of error in using the procedure. A few of the tests involved more general loading histories, with mixed loading amplitudes and rest periods between loads. Results and discussions of these tests are presented in Section IV.

## SECTION II

### A PRACTICAL PROCEDURE FOR REDUCTION OF SHEAR MODULUS WITH INCREASING STRAIN LEVEL.

#### 1. Objective

The objective of this section is to present the procedure recommended for reduction of shear modulus with increasing strain level in a practical form, for use in pavement evaluation, unencumbered by details of testing or presentation of the supporting data.

#### 2. Definitions

The following parameters are used and are defined with reference to figure 1:

**Maximum Shear Modulus =  $G_{\max}$**  = the initial tangent modulus, or secant modulus for strain amplitude  $\leq 10^{-5}$  in/in (For pavement evaluation this quantity is to be measured by the nondestructive vibratory test);

**Maximum Shear Stress =  $\tau_{\max}$**  = strength of the specimen in simple shear, defines asymptote in figure 1 (This quantity has been related empirically to  $G_{\max}$ , see Appendix I. However, if measured values of  $\tau_{\max}$  are used, a rate of loading corresponding to  $T = 0.1$  will suffice, eventhough the value of  $T$  for actual aircraft loading may be 0.01);

**Reference Strain =  $\gamma_r = \tau_{\max} / G_{\max}$** , defined by the intersection of the initial tangent line and strength asymptote in figure 1, and empirically related to  $G_{\max}$  in this section;

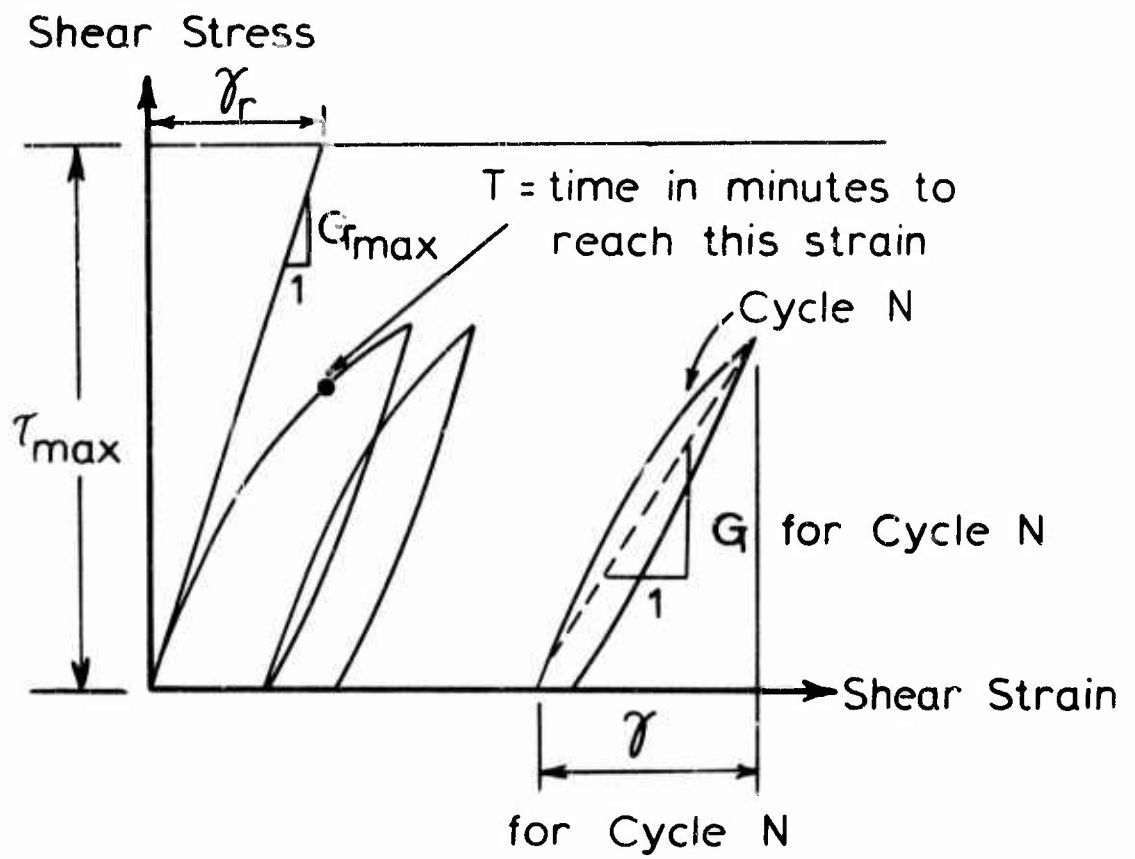


Figure 1. Schematic simple shear-stress strain relation.

Normalized Strain =  $\gamma/\gamma_r$ , where  $\gamma$  is the shear strain;

Hyperbolic Strain =  $\gamma_h$  a parameter defined by equation 9 (If equation 9 is substituted into equation 8, the relationship between normalized shear modulus and normalized strain is obtained. This relationship changes with the value of  $a$ , as shown in figure 15, depending on the values of  $S$ ,  $N$ ,  $T$ , and the type of soil; see equation 10. An alternate method of presentation is used in this section. Graphs based on equation 9 are presented giving the value of  $\gamma_h$  corresponding to a value of  $\gamma/\gamma_r$ , depending on the values of  $S$ ,  $N$ ,  $T$ , and soil type. With the value of  $\gamma_h$  determined, the normalized shear modulus is given by the simple hyperbolic equation 8.);

Shear Modulus =  $G$  = secant shear modulus for a given strain amplitude and cycle as shown in figure 1;

Normalized Shear Modulus =  $G/G_{\max}$ ;

Number of Cycles =  $N$ ;

Strain Time =  $T$  = time in minutes to reach a normalized strain equal to one;

Percent Saturation =  $S$  = ratio of volume of water to volume of voids in the soil, expressed as a percentage, and;

Void Ratio =  $e$  = ratio of volume of voids to volume of solids in the soil.

### 3. Determination of the Reference Strain

The reference strain is given by the following equation derived in

Appendix I.

$$\gamma_r = \frac{G_{\max}}{F^2 R^2} \left[ 0.6 - 0.25 (PI)^{0.6} \right] \quad (1)$$

where PI = plasticity index,  $G_{\max}$  is in psi,

$$F = \frac{(2.973 - e)^2}{(1 + e)} \quad (2)$$

$$\left. \begin{array}{l} R = 1100, \text{ for sands with less than 15 percent fines} \\ \text{and } R = 1100 - 6S, \text{ for cohesive soils with more than 15 percent fines} \end{array} \right\} (3)$$

Let

$$C_1 = \frac{F^2 R^2}{0.6 - 0.25 (PI)^{0.6}} \quad (4)$$

Then for sands with less than 15 percent fines, PI = 0 and R = 1100

giving

$$C_1 = (2.017 \times 10^6) F^2 \quad (5)$$

For cohesive soils with more than 15 percent fines, substituting R = 1100 - 6S

into equation 4

$$C_1 = \frac{F^2 (1100 - 6S)^2}{0.6 - 0.25 (PI)^{0.6}} \quad (6)$$

Finally

$$\gamma_r = \frac{G_{\max}}{C_1} \quad (7)$$

With  $G_{\max}$  in psi.

The value of  $C_1$  for sands with less than 15 percent fines, as defined by equations 2 and 5, is given in figure 2. The value of void ratio is all that is needed to determine  $C_1$  for this case. The value of  $C_1$  for cohesive soils with more than 15 percent fines, as defined by equations 2 and 6, is given in figure 3.

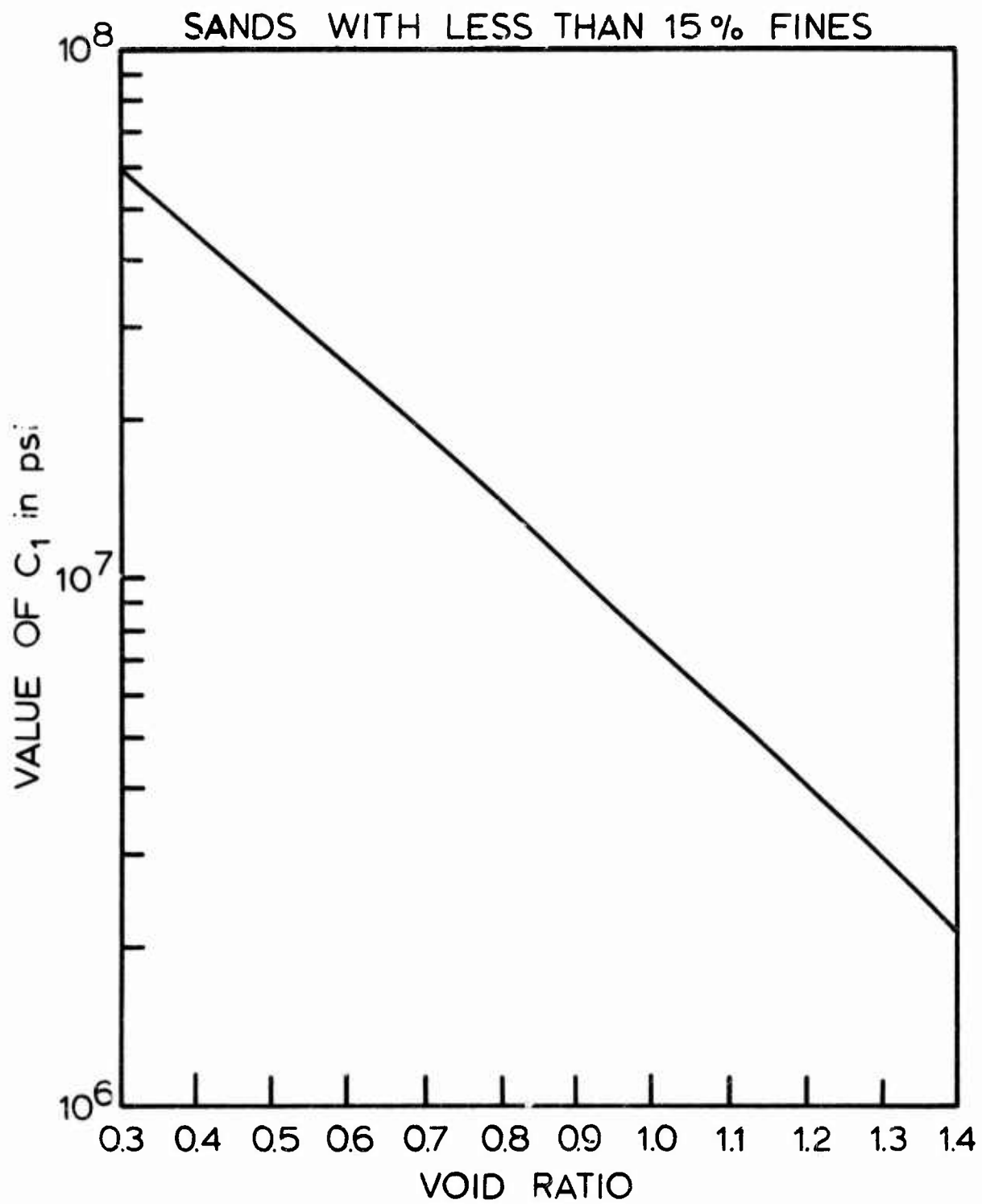


Figure 2. Value of  $C_1$  versus void ratio for sands with less than 15 percent fines.

For this case the values of the plasticity index and percent saturation are needed in addition to the value of the void ratio. The dashed line in figure 3 shows how to use the figure. First, using the left hand side of the graph with the value of plasticity index as abscissa, determine an ordinate depending on percent saturation. Extend this ordinate to the right to determine an abscissa for the right hand side of the graph, corresponding to the value of void ratio. The second abscissa determines the value of  $C_1$ . The dashed line represents the case where  $PI = 25$ ,  $S = 50$ , and  $e = 1$ . The value of  $C_1 = 4.9 \times 10^6$  psi.

Having determined the value of  $C_1$  from either figure 2 or figure 3, depending on the soil type, the reference strain can now be determined from figure 4. Using the value of  $C_1$  as abscissa, the value of the reference strain is read as ordinate, from the curve corresponding to the value of  $G_{max}$  in psi. The dashed lines in figure 4 are for  $C_1 = 4.9 \times 10^6$  psi and  $G_{max} = 8000$  psi,  $\gamma_r = 16.5 \times 10^{-4}$  in/in.

#### 4. Determination of the Shear Modulus

The normalized shear modulus is given by

$$\frac{G}{G_{max}} = \frac{1}{1 + \gamma_h} \quad (8)$$

where

$$\gamma_h = \frac{\gamma}{\gamma_r} \left[ 1 + a e_{xp} - \left[ \frac{\gamma}{\gamma_r} \right]^{0.4} \right] \quad (9)$$

The value of  $a$  is defined by one of the following equations, depending on the type of soil

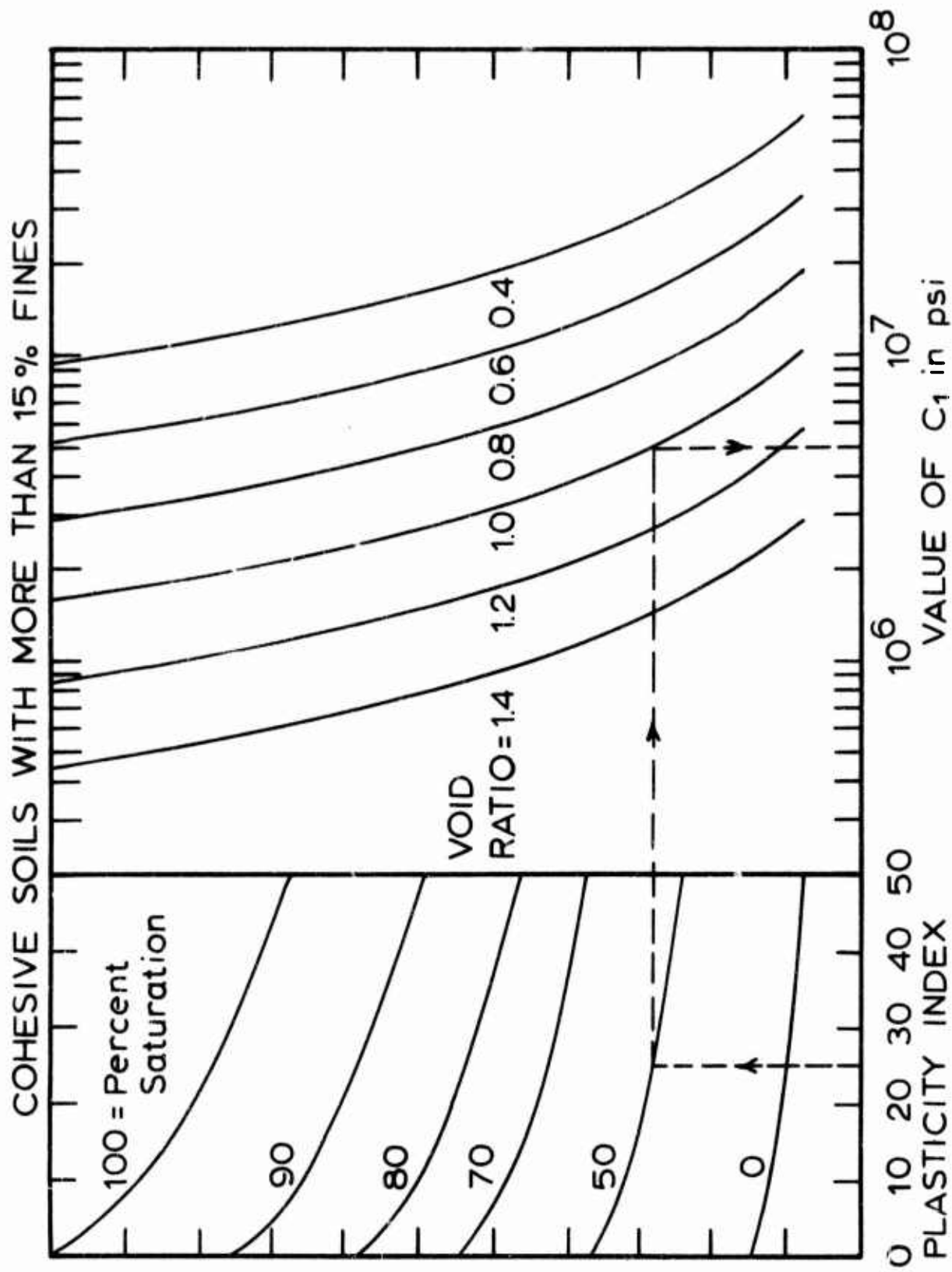


Figure 3. Value of  $C_1$  versus plasticity index, percent saturation, and void ratio for cohesive soils with more than 15 percent fines.

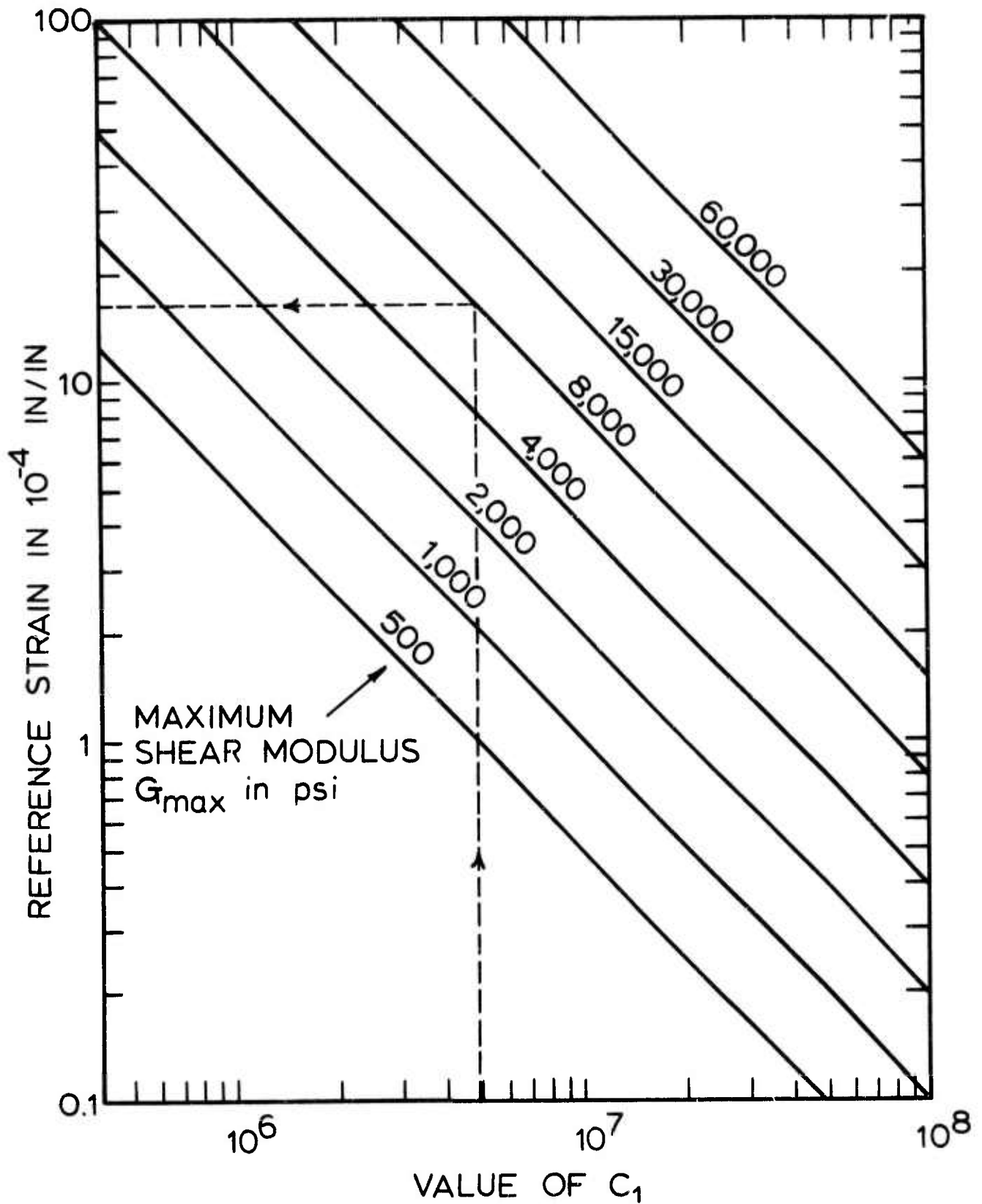


Figure 4. Reference strain versus value of  $C_1$  and maximum shear modulus.

$$a = \left\{ \begin{array}{ll} [(3.85/N) - 0.85] T^{0.025} & \text{for clean dry sands} \\ 1.6(1 + 0.02S) T^{0.2} / N^{0.6} & \text{for nonplastic soils with} \\ & \text{fines and low plasticity} \\ & \text{soils} \\ 0.2(1 + 0.02S) T^{0.75} / N^{0.15} & \text{for high plasticity soils} \\ & \text{with liquid limit } > 50 \end{array} \right\} \quad (10)$$

The values of  $\gamma_h$  as defined by equations 9 and 10 are given in figures 5, 6, 7 and 8 for various cases. Figure 5 is for clean dry sands. The solid curves give the relationship between  $\gamma_h$  and  $\gamma/\gamma_r$  for a fast rate of loading,  $T = 0.01$ . The dashed curves are for a slow rate of loading,  $T = 10$ . Curves are shown for  $N = 1, 2, 10, > 100$ . The dashed and solid curves coincide for 10 and  $> 100$  cycles. Having determined the reference strain according to the procedure given in paragraph 2, the normalized strain can be computed, and the hyperbolic strain determined from figure 5 for clean dry sands. Similar graphs are given in figures 6 and 7 for nonplastic soils with fines and low plasticity soils. In figures 6 and 7 the solid curves are for 60 percent saturation and the dashed curves are for 100 percent saturation. Figure 6 is for a fast rate of loading,  $T = 0.01$ , and figure 7 is for a slow rate of loading,  $T = 10$ . Both sets of curves in figures 6 and 7 approach the hyperbolic line for a large number of cycles. Again, knowing the value of reference strain, the value of the hyperbolic strain can be determined from these figures for a given value of strain. Figure 8 is a similar graph for high plasticity soils. For the fast rate of loading,  $T = 0.01$ , the hyperbolic line defines the relationship for all numbers of cycles and percent's saturation. For the slow rate of loading,  $T = 10$ , the solid curves define the relationship for 60 percent saturation, and the dashed curves

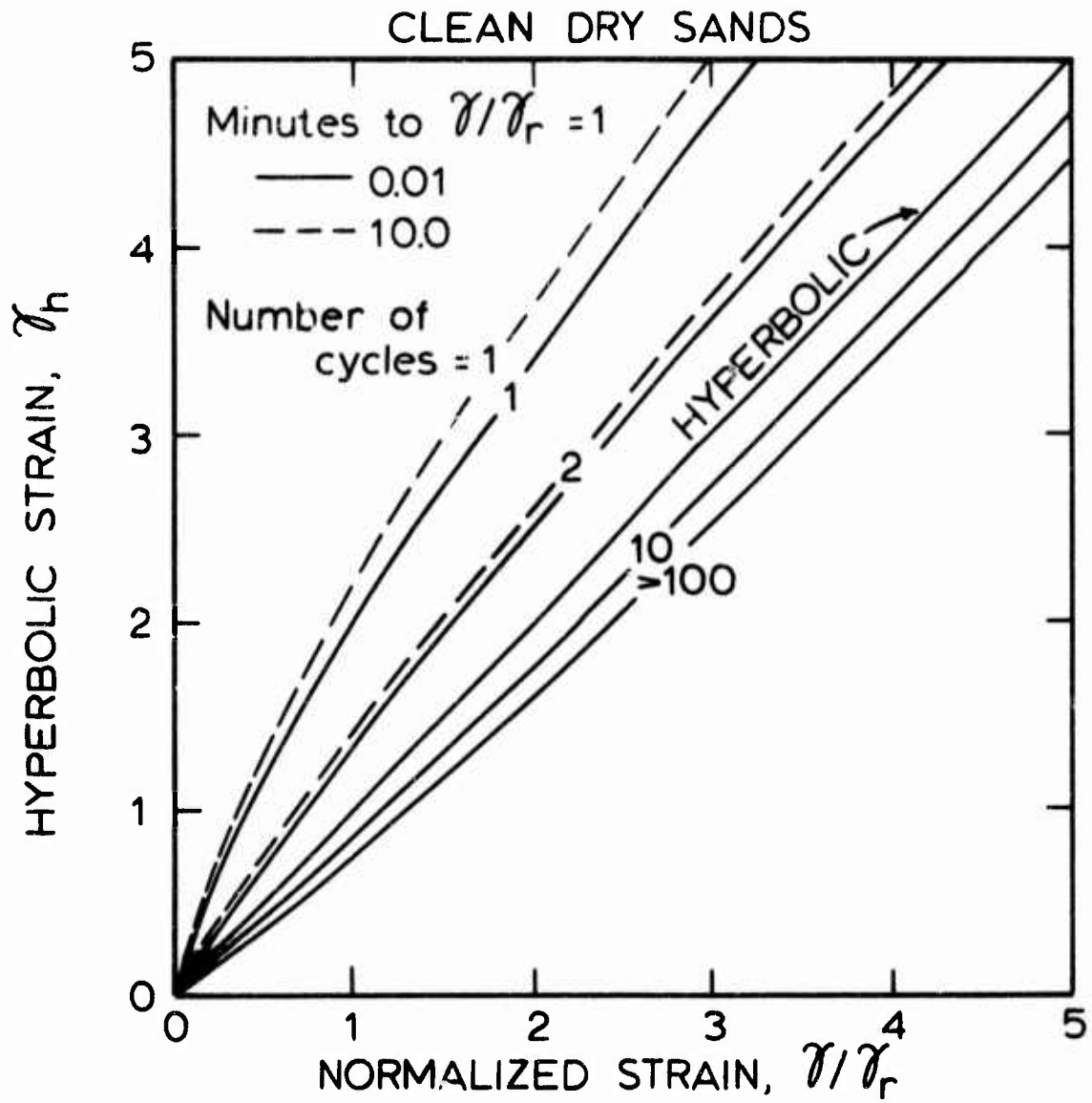


Figure 5. Hyperbolic strain versus normalized strain for various numbers of cycles and rates of loading.

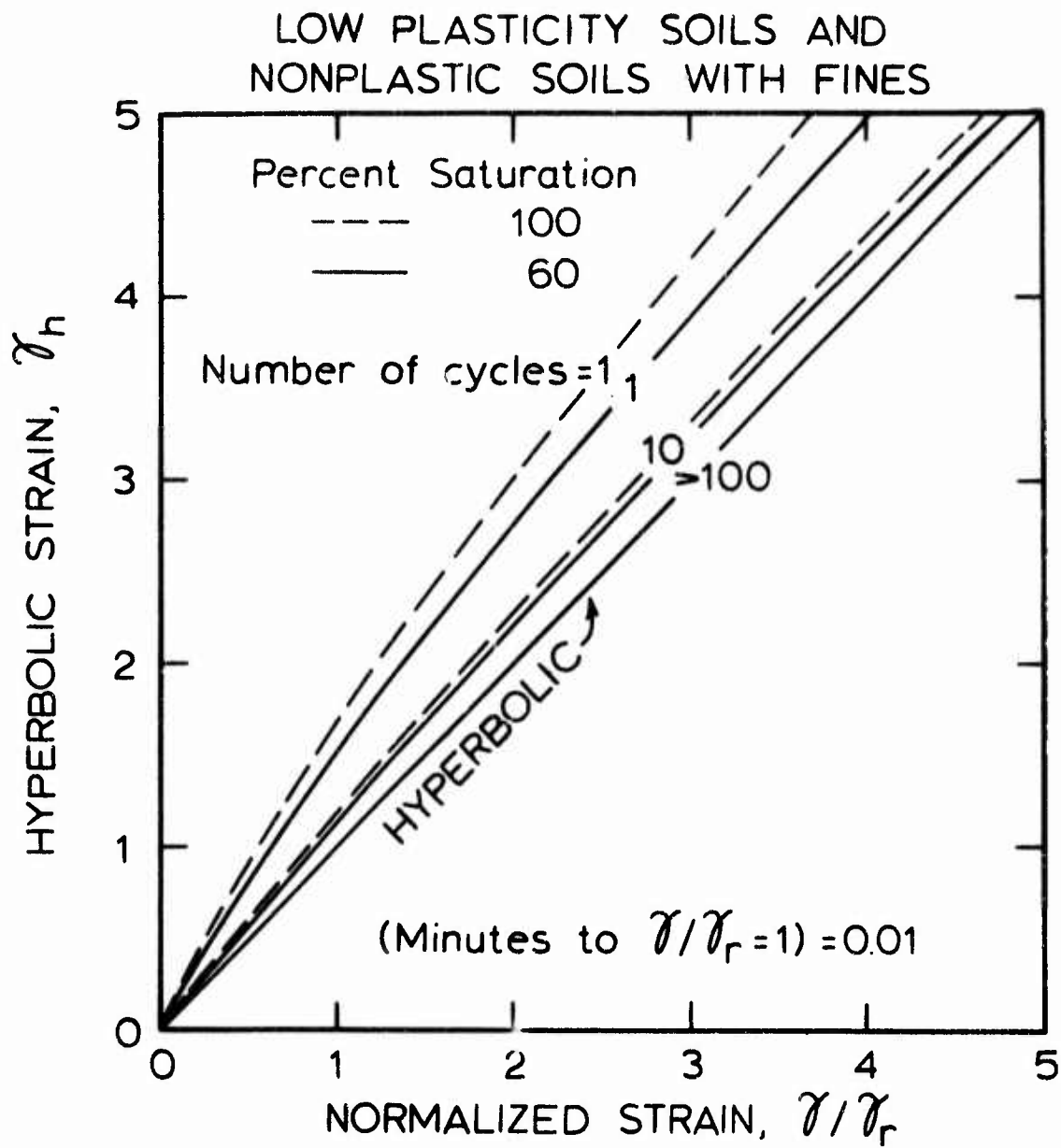


Figure 6. Hyperbolic strain versus normalized strain for various numbers of cycles and percents saturation, slow rate of loading,  $T = 0.01$ , nonplastic soils with fines and low plasticity soils.

LOW PLASTICITY SOILS AND  
NONPLASTIC SOILS WITH FINES

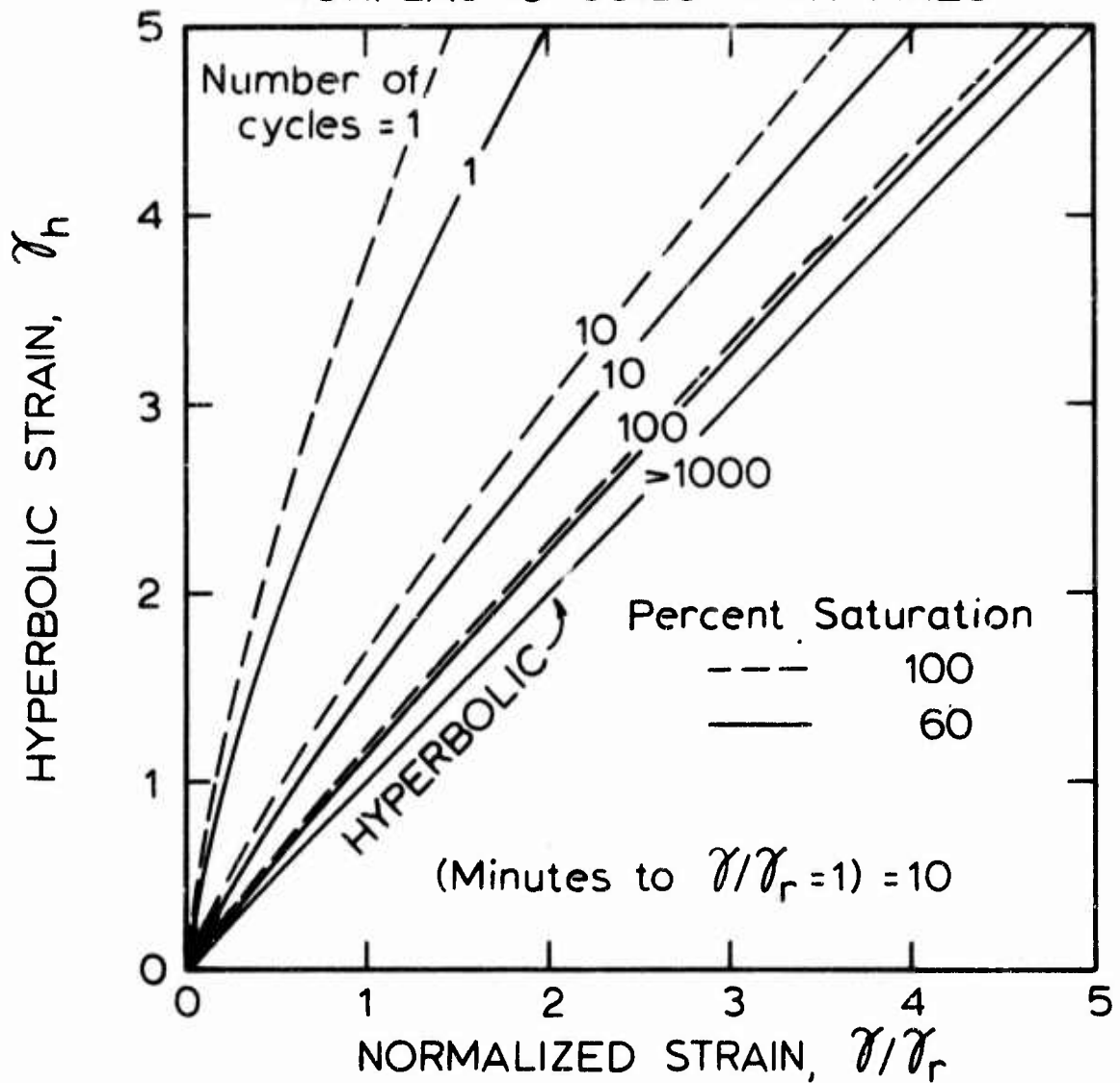


Figure 7. Hyperbolic strain versus normalized strain for various numbers of cycles and percents saturation, slow rate of loading,  $T = 10$ , nonplastic soils with fines and low plasticity soils.

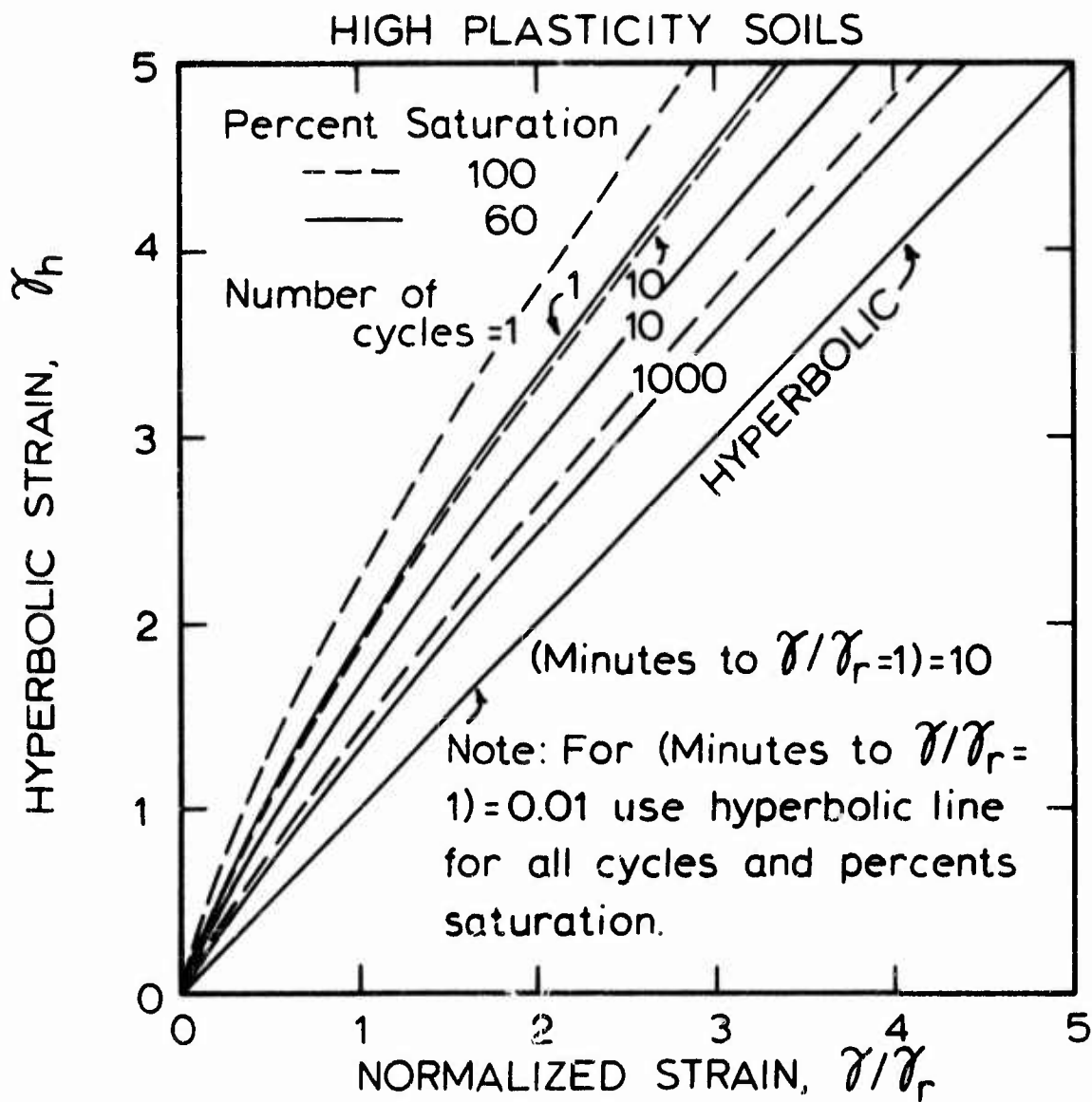


Figure 8. Hyperbolic strain versus normalized strain for numbers of cycles, percents saturation, and rates of loading, high plasticity soils.

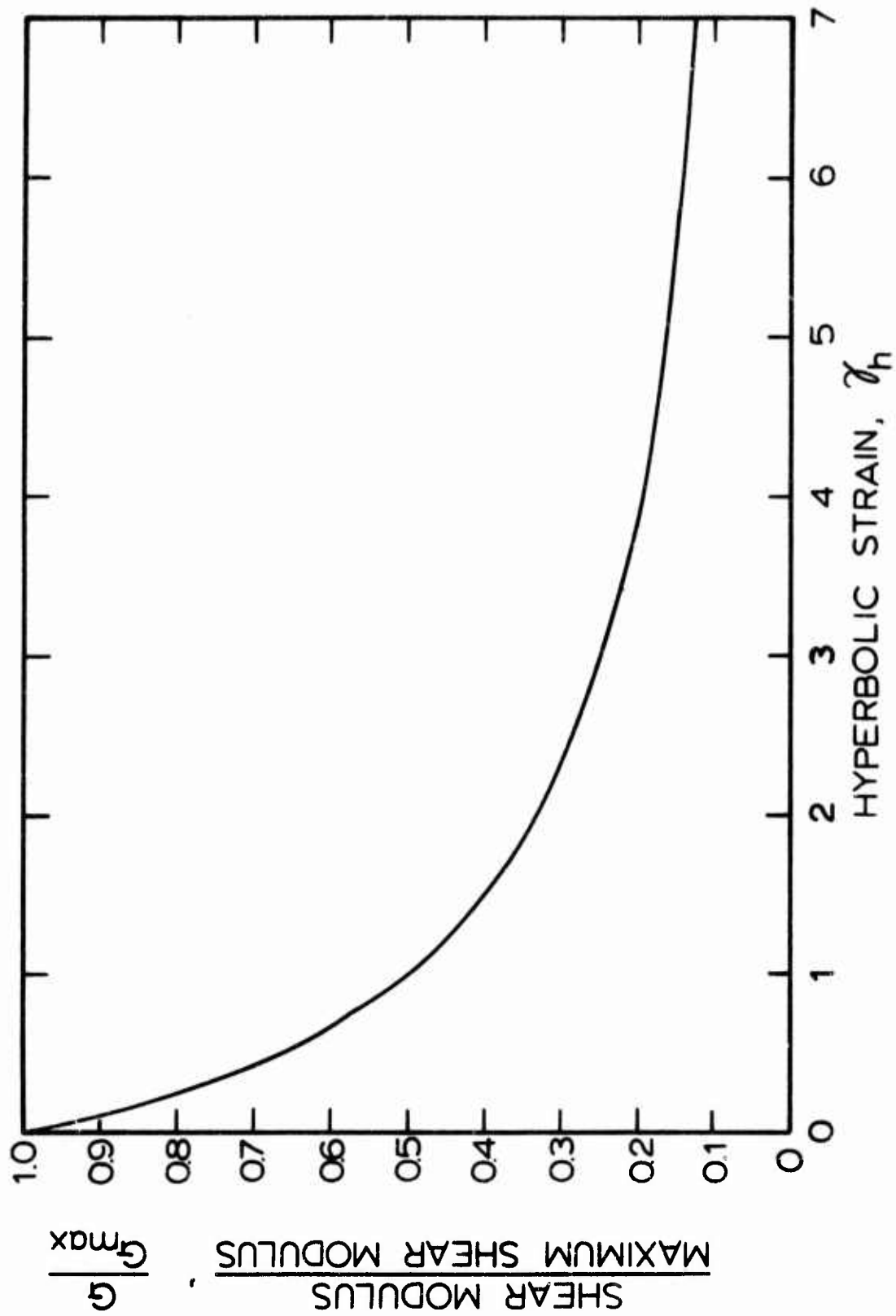


Figure 9. Normalized shear modulus versus hyperbolic strain.

are for 100 percent saturation. With the value of hyperbolic strain determined from one of figures 5, 6, 7, or 8, depending on soil type, the normalized shear modulus can be determined from figure 9.

5. Examples of Use of the Procedure

For pavement evaluation the type of soil (including PI and particle size) and values of  $e$  and  $S$  would have to be estimated from available knowledge of the subgrade or from a core sample; the value of  $G_{\max}$  would be measured by nondestructive vibratory testing; the value of  $N$  would come from traffic records; the value of  $\gamma$  would be determined by the finite-element analysis, and; the value of  $T$  would depend on the speed of the aircraft.

Example number 1:

Given: A clean dry sand,

$$G_{\max} = 18380 \text{ psi,}$$

$$e = 0.62,$$

$$N = 1,$$

$$\gamma = 18.6 \times 10^{-4} \text{ in/in,}$$

$$T = 81 \text{ (a very slow rate of loading).}$$

Find: The shear modulus,  $G$ ;

From figure 2, using  $e = 0.62$ ;  $C_1 = 2.36 \times 10^7$  psi.

From figure 4, using  $C_1 = 2.36 \times 10^7$  and  $G_{\max} = 18380$  psi;

$$\gamma_r = 7.5 \times 10^{-4} \text{ in/in.}$$

Calculate, using  $\gamma = 18.6 \times 10^{-4}$  and  $\gamma_r = 7.5 \times 10^{-4}$ ;

$$\gamma/\gamma_r = (18.6 \times 10^{-4}) / (7.5 \times 10^{-4}) = 2.48.$$

From figure 5, using  $\gamma/\gamma_r = 2.48$ ,  $N = 1$ , and  $T = 81$ ;

$$\gamma_h = 4.4$$

From figure 9, using  $\gamma_h = 4.4$ ;  $G/G_{\max} = 0.185$

Calculate, using  $G/G_{\max} = 0.185$  and  $G_{\max} = 18380$  psi;

$$G = (0.185) (18380) = 3400 \text{ psi}$$

The same parameters given in this example were measured for test no. 101 of the WES Sand (see figure 16). The measured shear modulus,  $G = 3320$  psi, in this case, was less than 3 percent difference between calculated and measured values.

Example number 2:

Given: A low plasticity soil,

$$PI = 6,$$

Percent passing no. 200 sieve = 96,

$$G_{\max} = 12680 \text{ psi},$$

$$e = 0.67,$$

$$S = 73,$$

$$N = 10,$$

$$\gamma = 12.9 \times 10^{-4} \text{ in/in},$$

$T = 0.38$  (a medium fast rate of loading).

Find: The shear modulus,  $G$ ;

From figure 3, using  $PI = 6$ ,  $S = 73$ , and  $e = 0.67$ ;

$$C_1 = 8.0 \times 10^6 \text{ psi.}$$

From figure 4, using  $C_1 = 8.0 \times 10^6$  psi and  $G_{\max} = 12680$  psi;

$$\gamma_r = 15 \times 10^{-4} \text{ in/in.}$$

Calculate, using  $\gamma = 12.9 \times 10^{-4}$  and  $\gamma_r = 15 \times 10^{-4}$ ;

$$\gamma/\gamma_r = (12.9 \times 10^{-4}) / (15 \times 10^{-4}) = 0.860.$$

Since  $T = 0.38$ , use the average between figures 6 and 7,

also using  $\gamma/\gamma_r = 0.860$ ,  $N = 10$ , and  $S = 73$ ;

$$\gamma_h = [(1.0 \text{ from figure 6}) + (1.44 \text{ from figure 7})] / 2 = 1.22.$$

From figure 9, using  $\gamma_h = 1.22$ ;  $G/C_{\max} = 0.450$

Calculate, using  $G/G_{\max} = 0.450$  and  $G_{\max} = 12680 \text{ psi}$ ;

$$G = (0.450) (12680) = 5700 \text{ psi}$$

The same parameters given in this example were measured for test no. 27 of the Vicksburg Loess. The measured shear modulus  $G = 5580 \text{ psi}$ , in this case, was less than 3 percent difference between calculated and measured values. Not all cases would compare this well, but these were not chosen specifically to show a good comparison.

### SECTION III

#### COMPARISON OF VALUES FROM THE PRACTICAL PROCEDURE TO EXPERIMENTAL DATA

##### 1. Soils Tested

Classification data for each of the soils tested and various test parameters for each of the tests are given in tables 1, 2, 3, and 4. In these tables the soils are grouped into four different categories. Table 1 gives data for clean sands and other sands with high permeability. Table 2 gives data for nonplastic silty sands. Table 3 gives data for low plasticity soils and table 4 for high plasticity soils. The particle size distribution curves for these soils are given in figures 10, 11, and 12. Those in figure 10 are for nonplastic soils, corresponding to the soils in tables 1 and 2. Figure 11 is for low plasticity soils, corresponding to table 3, and figure 12 is for high plasticity soils, corresponding to table 4. Study of these tables and figures will show that the testing program covered a wide variety of soil types and large ranges of test parameters.

##### 2. Values of R for Determination of Reference Strain

Rearranging equation 16 in Appendix I gives

$$R = \frac{G_{\max}}{F} \left[ \frac{0.6 - 0.25 (PI)^{0.6}}{\tau_{\max}} \right]^{1/2} \quad (11)$$

For each test, using the measured values of PI, e,  $\tau_{\max}$ , and  $G_{\max}$ , a measured value of R can be calculated with equations 2 and 11. In figures 13 and 14 measured values of R for 22 of the soils tested are compared to values calculated with the second of equation 3, for cohesive soils with more than 15 percent fines. In general, equation 3 is a fairly good representation of the

Table 1. Data for Simple Shear Tests of Clean Sands and Other Sands with High Permeability.

WES SAND  
NUMBER OF TESTS = 10  
PERCENT PASSING NO. 200 SIEVE = 0.  
PLASTICITY INDEX = NP  
LIQUID LIMIT = NP

TEST NO.	RECORD NO.	VOID RATIO	PERCENT SATURATION	CHAMBER PRESSURE KG/SQ CM	PRINCIPAL STRESS DIFFERENCE KG/SQ CM	INITIAL MAX G PSI	RECOVERY MAX G PSI	CYCLES BEFORE RECOVERY	SHEAR STRESS INCREMENT KG/SQ CM	MAXIMUM SHEAR STRESS KG/SQ CM	SHEAR STRESS RATIO	LOAD RATE KG/SQ CM PER HOUR
(1)	(2)	(3)	(4)	(5)	(6)	(7)	(8)	(9)	(10)	(11)	(12)	(13)
34	1	0.65	0.	1.0	0.127	12010.	10840.	2700	0.297	0.521	0.4035	57.903
35	1	0.66	0.	1.0	0.115	10200.	10200.	1001	0.476	0.899	0.5297	74.072
36	1	0.68	0.	1.0	0.127	12030.	12730.	2900	0.101	0.570	0.2873	39.834
37	1	0.69	0.	1.0	0.127	11900.	13810.	1600	0.343	0.538	0.6374	40.230
38	1	0.67	0.	1.0	0.115	10270.	10240.	695	0.627	0.915	0.6847	37.131
39	1	0.70	0.	1.0	0.115	10600.	10900.	202	0.323	1.039	0.3104	36.747
83	1	0.64	0.	1.0	0.080	15300.	20000.	9435	0.462	0.913	0.5066	369.989
84	1	0.64	0.	1.0	0.115	10640.	10640.	1	0.451	0.981	0.4596	0.222
101	1	0.62	0.	1.0	0.110	10300.	10170.	19	0.469	0.962	0.4671	0.227
112	1	0.67	0.	1.0	0.087	10310.	17160.	320	0.462	0.909	0.5087	17.297

ST. JOHNS SAND  
NUMBER OF TESTS = 4  
PERCENT PASSING NO. 200 SIEVE = 14.  
PLASTICITY INDEX = NP  
LIQUID LIMIT = NP

TEST NO.	RECORD NO.	VOID RATIO	PERCENT SATURATION	CHAMBER PRESSURE KG/SQ CM	PRINCIPAL STRESS DIFFERENCE KG/SQ CM	INITIAL MAX G PSI	RECOVERY MAX G PSI	CYCLES BEFORE RECOVERY	SHEAR STRESS INCREMENT KG/SQ CM	MAXIMUM SHEAR STRESS KG/SQ CM	SHEAR STRESS RATIO	LOAD RATE KG/SQ CM PER HOUR
(1)	(2)	(3)	(4)	(5)	(6)	(7)	(8)	(9)	(10)	(11)	(12)	(13)
76	1	0.78	100.	0.5	0.090	12500.	11690.	4003	0.196	0.304	0.5989	22.201
77	1	0.81	100.	3.0	0.034	20100.	27900.	1114	0.540	2.511	0.2182	24.148
79	1	0.65	88.	1.5	0.076	21400.	21760.	2155	0.211	1.610	0.1309	38.032
80	1	0.64	98.	1.0	0.088	16930.	17570.	2100	0.427	1.280	0.3387	24.994

Table 2. Data for Simple Shear Tests of Nonplastic Silty Sands.

DOVER  
NUMBER OF TESTS = 5  
PERCENT PASSING NO. 200 SIEVE = 42.  
PLASTICITY INDEX = NP  
LIQUID LIMIT = NP

TEST NO.	RECORD NO.	VOID RATIO	PERCENT SATURATION	CHAMBER PRESSURE KG/SQ CM	PRINCIPAL STRESS DIFFERENCE KG/SQ CM	INITIAL MAX G PSI	RECOVERY MAX G PSI	CYCLES BEFORE RECOVERY	SHEAR STRESS INCREMENT KG/SQ CM	MAXIMUM SHEAR STRESS KG/SQ CM	SHEAR STRESS RATIO	LOAD RATE KG/SQ CM PER HOUR
(1)	(2)	(3)	(4)	(5)	(6)	(7)	(8)	(9)	(10)	(11)	(12)	(13)
54	1	0.53	96.	0.5	0.098	10610.	10610.	1039	0.430	1.009	0.4364	25.435
56	1	0.45	93.	0.5	0.100	17290.	31210.	608	0.225	0.916	0.2459	10.664
57	1	0.41	98.	1.0	0.088	19770.	22610.	1260	0.425	1.734	0.2449	43.226
58	1	0.36	79.	1.0	0.088	22000.	25020.	646	0.420	1.405	0.3065	31.561
59	1	0.42	59.	0.5	0.098	15690.	18390.	811	0.538	0.929	0.5791	41.126

PRESTONSBURG SAND  
NUMBER OF TESTS = 4  
PERCENT PASSING NO. 200 SIEVE = 34.  
PLASTICITY INDEX = NP  
LIQUID LIMIT = NP

TEST NO.	RECORD NO.	VOID RATIO	PERCENT SATURATION	CHAMBER PRESSURE KG/SQ CM	PRINCIPAL STRESS DIFFERENCE KG/SQ CM	INITIAL MAX G PSI	RECOVERY MAX G PSI	CYCLES BEFORE RECOVERY	SHEAR STRESS INCREMENT KG/SQ CM	MAXIMUM SHEAR STRESS KG/SQ CM	SHEAR STRESS RATIO	LOAD RATE KG/SQ CM PER HOUR
(1)	(2)	(3)	(4)	(5)	(6)	(7)	(8)	(9)	(10)	(11)	(12)	(13)
72	1	0.59	37.	0.5	0.098	15460.	17050.	2999	0.317	0.783	0.4664	38.814
73	1	0.50	36.	1.0	0.088	12710.	21780.	1560	0.562	0.952	0.5904	38.050
74	1	0.59	47.	0.7	0.094	11220.	20000.	850	0.583	0.798	0.7106	10.552
75	1	0.54	49.	1.0	0.076	21650.	17490.	650	0.520	1.290	0.4032	17.970

Table 2. Data for Simple Shear Tests of Nonplastic Silty Sands (cont').

KENTLAND NO. 10-25 NUMBER OF TESTS = 5 PERCENT PASSING NO. 200 SIEVE = 36. PLASTICITY INDEX = NP LIQUID LIMIT = NP												
TEST NO.	RECORD NO.	VOID RATIO	PERCENT SATURATION	CHAMBER PRESSURE KG/50 CM	PRINCIPAL STRESS DIFFERENCE KG/50 CM	INITIAL MAX. G. PSI	RECOVERY MAX. G. PSI	CYCLES BEFORE RECOVERY	SHEAR STRESS INCREMENT KG/50 CM	MAXIMUM SHEAR STRESS KG/50 CM	SHEAR STRESS RATIO	LOAD RATE KG/50 CM PER HOUR
111	121	1.31	101	1.0	101	171	191	191	1101	1111	1111	1111
112	1	2.04	75	1.0	0.008	12235.	13700.	1004	0.293	0.027	0.4000	21.095
113	1	0.91	92	1.0	0.008	16100.	17300.	716	0.255	0.495	0.5008	15.928
114	1	0.81	91	1.0	0.008	12070.	12270.	974	0.226	0.451	0.4820	20.117
115	1	0.91	92	1.0	0.008	14810.	16432.	677	0.209	0.769	0.3629	31.676
KENTLAND NO. 10-35 NUMBER OF TESTS = 4 PERCENT PASSING NO. 200 SIEVE = 44. PLASTICITY INDEX = NP LIQUID LIMIT = NP												
TEST NO.	RECORD NO.	VOID RATIO	PERCENT SATURATION	CHAMBER PRESSURE KG/50 CM	PRINCIPAL STRESS DIFFERENCE KG/50 CM	INITIAL MAX. G. PSI	RECOVERY MAX. G. PSI	CYCLES BEFORE RECOVERY	SHEAR STRESS INCREMENT KG/50 CM	MAXIMUM SHEAR STRESS KG/50 CM	SHEAR STRESS RATIO	LOAD RATE KG/50 CM PER HOUR
116	121	1.31	101	1.0	101	171	191	191	1101	1111	1111	1111
117	1	2.04	50	1.0	0.008	22900.	22900.	2051	0.499	1.322	0.3634	76.190
118	1	0.95	55	1.0	0.007	19570.	19570.	879	0.452	1.020	0.4631	10.909
119	1	0.92	50	1.0	0.007	20000.	20000.	2665	0.336	1.092	0.3073	79.187
120	1	2.71	60	1.0	0.007	12840.	14640.	760	0.557	0.952	0.5068	41.147
KENTLAND NO. 4-12 NUMBER OF TESTS = 4 PERCENT PASSING NO. 200 SIEVE = 10. PLASTICITY INDEX = NP LIQUID LIMIT = NP												
TEST NO.	RECORD NO.	VOID RATIO	PERCENT SATURATION	CHAMBER PRESSURE KG/50 CM	PRINCIPAL STRESS DIFFERENCE KG/50 CM	INITIAL MAX. G. PSI	RECOVERY MAX. G. PSI	CYCLES BEFORE RECOVERY	SHEAR STRESS INCREMENT KG/50 CM	MAXIMUM SHEAR STRESS KG/50 CM	SHEAR STRESS RATIO	LOAD RATE KG/50 CM PER HOUR
121	121	1.31	101	1.0	101	171	191	191	1101	1111	1111	1111
122	1	0.90	30	1.0	0.007	12010.	12000.	1041	0.369	0.860	0.3983	62.122
123	1	0.95	36	1.0	0.007	10080.	10080.	801	0.313	0.825	0.4021	19.006
124	1	0.93	40	1.0	0.007	13050.	13050.	104	0.407	0.941	0.4329	4.311
125	1	0.93	30	1.0	0.007	13000.	13000.	930	0.411	0.820	0.4904	26.439
KENTLAND NO. 4-30 NUMBER OF TESTS = 2 PERCENT PASSING NO. 200 SIEVE = 30. PLASTICITY INDEX = NP LIQUID LIMIT = NP												
TEST NO.	RECORD NO.	VOID RATIO	PERCENT SATURATION	CHAMBER PRESSURE KG/50 CM	PRINCIPAL STRESS DIFFERENCE KG/50 CM	INITIAL MAX. G. PSI	RECOVERY MAX. G. PSI	CYCLES BEFORE RECOVERY	SHEAR STRESS INCREMENT KG/50 CM	MAXIMUM SHEAR STRESS KG/50 CM	SHEAR STRESS RATIO	LOAD RATE KG/50 CM PER HOUR
126	121	1.31	101	1.0	101	171	191	191	1101	1111	1111	1111
127	1	0.41	70	1.0	0.007	21900.	20650.	1299	0.371	1.019	0.3693	16.111
128	1	0.98	55	1.0	0.007	20970.	21070.	474	0.531	0.753	0.7047	10.596
KENTLAND NO. 7-15 NUMBER OF TESTS = 2 PERCENT PASSING NO. 200 SIEVE = 45. PLASTICITY INDEX = NP LIQUID LIMIT = NP												
TEST NO.	RECORD NO.	VOID RATIO	PERCENT SATURATION	CHAMBER PRESSURE KG/50 CM	PRINCIPAL STRESS DIFFERENCE KG/50 CM	INITIAL MAX. G. PSI	RECOVERY MAX. G. PSI	CYCLES BEFORE RECOVERY	SHEAR STRESS INCREMENT KG/50 CM	MAXIMUM SHEAR STRESS KG/50 CM	SHEAR STRESS RATIO	LOAD RATE KG/50 CM PER HOUR
129	121	1.31	101	1.0	101	171	191	191	1101	1111	1111	1111
130	1	2.07	36	1.0	0.007	10500.	13000.	900	0.365	0.914	0.3993	13.987
131	1	0.66	34	1.0	0.007	14070.	14000.	1972	0.500	1.204	0.4154	73.944
KENTLAND NO. 7-27 NUMBER OF TESTS = 2 PERCENT PASSING NO. 200 SIEVE = 24. PLASTICITY INDEX = NP LIQUID LIMIT = NP												
TEST NO.	RECORD NO.	VOID RATIO	PERCENT SATURATION	CHAMBER PRESSURE KG/50 CM	PRINCIPAL STRESS DIFFERENCE KG/50 CM	INITIAL MAX. G. PSI	RECOVERY MAX. G. PSI	CYCLES BEFORE RECOVERY	SHEAR STRESS INCREMENT KG/50 CM	MAXIMUM SHEAR STRESS KG/50 CM	SHEAR STRESS RATIO	LOAD RATE KG/50 CM PER HOUR
132	121	1.31	101	1.0	101	171	191	191	1101	1111	1111	1111
133	1	0.24	32	1.0	0.007	10150.	9150.	2556	0.303	0.865	0.3673	52.463
134	1	0.24	31	1.0	0.007	14410.	16100.	306	0.300	1.030	0.1691	2.422

Table 3. Data for Simple Shear Tests of Low Plasticity Soils.

A14 FINE SILTY SAND  
NUMBER OF TESTS = 17  
PERCENT PASSING NO. 200 SIEVE = 62.  
PLASTICITY INDEX = 0.  
LIQUID LIMIT = 19.

TEST NO.	RECORD NO.	VOID RATIO	PERCENT SATURATION	CHAMBER PRESSURE KG/SQ CM	PRINCIPAL STRESS DIFFERENCE KG/SQ CM	INITIAL MAX G PSI	RECOVERY MAX G PSI	CYCLES OFF/RECOVERY	SHEAR STRESS INCREMENT KG/SQ CM	MAXIMUM SHEAR STRESS KG/SQ CM	SHEAR STRESS RATIO	LOAD RATE KG/SQ CM PER HOUR
(11)	(12)	(13)	(14)	(15)	(16)	(17)	(18)	(19)	(20)	(21)	(22)	(23)
1	1	0.57	45.	0.5	0.125	9750.	10900.	12	0.038	0.573	0.0663	0.109
2	2	0.56	45.	0.5	0.125	11800.	12900.	27	0.100	0.573	0.1943	0.176
3	3	0.56	45.	0.5	0.125	12500.	14000.	9	0.108	0.573	0.5372	0.205
4	4	0.56	45.	1.0	0.113	10750.	11900.	10	0.050	0.462	0.0981	0.176
5	5	0.56	45.	1.0	0.113	10800.	10900.	20	0.159	0.462	0.1866	0.157
6	6	0.56	45.	1.0	0.113	10800.	10900.	45	0.433	0.462	0.5027	0.131
7	7	0.57	41.	0.5	0.125	10450.	12000.	27	0.100	0.573	0.1866	0.242
8	8	0.57	41.	0.5	0.125	12110.	12700.	17	0.303	0.573	0.5283	0.223
9	9	0.57	41.	1.0	0.113	10900.	11710.	26	0.050	0.462	0.0582	0.167
10	10	0.57	41.	1.0	0.113	10900.	10970.	19	0.154	0.462	0.1704	0.148
11	11	0.57	41.	1.0	0.113	11900.	11100.	19	0.417	0.462	0.4037	0.114
12	12	0.57	41.	1.0	0.113	11900.	11200.	18	0.424	0.462	0.4918	0.119
13	13	0.57	33.	0.5	0.125	8050.	10230.	17	0.317	0.450	0.6926	0.235
14	14	0.57	33.	1.0	0.113	13600.	14150.	23	0.046	0.740	0.0655	0.384
15	15	0.57	33.	1.0	0.113	13260.	13320.	15	0.426	0.740	0.5756	0.319
16	16	0.57	42.	0.5	0.125	7620.	12070.	826	0.307	0.573	0.5363	26.155
17	17	0.57	42.	1.0	0.113	16900.	16900.	513	0.048	0.462	0.0582	38.139
18	18	0.57	42.	1.0	0.113	16900.	16910.	120	0.151	0.462	0.1748	38.957
19	19	0.57	42.	1.0	0.113	16110.	16110.	595	0.424	0.462	0.4921	32.536
20	20	0.57	39.	1.0	0.113	13360.	15150.	836	0.438	0.462	0.5097	33.642
21	21	0.51	53.	0.5	0.125	11800.	15760.	100	0.510	0.637	0.8004	39.148
22	22	0.53	52.	1.0	0.113	15160.	15920.	800	0.611	0.443	0.6476	46.294
23	23	0.48	82.	0.5	0.125	12300.	13930.	1261	0.374	0.636	0.5701	42.543
24	24	0.49	62.	0.5	0.125	11130.	13530.	2167	0.210	0.671	0.3127	42.713
25	25	0.51	55.	0.5	0.125	10410.	12680.	1130	0.106	0.669	0.1585	20.172
26	26	0.50	57.	1.0	0.113	15820.	16360.	935	0.217	0.995	0.2182	44.493
27	27	0.52	59.	0.5	0.125	11360.	13230.	120	0.518	0.707	0.7327	25.801
28	28	0.44	95.	0.5	0.098	4170.	4170.	1	0.289	0.269	1.0010	41.659
29	29	0.45	100.	0.5	0.098	4050.	4050.	1011	0.010	0.406	0.0251	4.106
30	30	0.45	100.	0.5	0.098	7600.	7600.	1492	0.107	0.463	0.2107	26.805
31	31	0.45	100.	0.5	0.098	7600.	6970.	1077	0.233	0.513	0.4542	40.512
32	32	0.39	96.	1.0	0.115	14930.	19930.	18	VAR	1.238	0.0000	VAR
33	33	0.39	76.	2.0	0.923	26130.	26130.	9	VAR	2.475	0.0000	VAR
34	34	0.40	74.	0.5	0.126	4320.	3620.	84	VAR	0.909	0.0000	VAR
35	35	0.41	87.	1.0	0.094	15570.	16600.	90	VAR	1.002	0.0000	VAR

A14 FINE SILTY CLAY  
NUMBER OF TESTS = 16  
PERCENT PASSING NO. 200 SIEVE = 86.  
PLASTICITY INDEX = 11.  
LIQUID LIMIT = 36.

TEST NO.	RECORD NO.	VOID RATIO	PERCENT SATURATION	CHAMBER PRESSURE KG/SQ CM	PRINCIPAL STRESS DIFFERENCE KG/SQ CM	INITIAL MAX G PSI	RECOVERY MAX G PSI	CYCLES OFF/RECOVERY	SHEAR STRESS INCREMENT KG/SQ CM	MAXIMUM SHEAR STRESS KG/SQ CM	SHEAR STRESS RATIO	LOAD RATE KG/SQ CM PER HOUR
(11)	(12)	(13)	(14)	(15)	(16)	(17)	(18)	(19)	(20)	(21)	(22)	(23)
16	1	0.72	57.	0.5	0.098	7170.	8250.	849	0.014	0.851	0.0166	7.182
16	2	0.72	57.	0.5	0.098	7650.	8650.	1668	0.181	0.851	0.2124	41.866
16	3	0.72	57.	0.5	0.098	8960.	8960.	460	0.541	0.851	0.6360	48.366
17	1	0.72	55.	0.5	0.098	7740.	8750.	2004	0.313	0.831	0.3762	56.789
18	1	0.72	54.	0.5	0.098	7140.	7100.	85	0.626	0.763	0.8209	54.428
19	1	0.72	55.	1.0	0.087	9140.	11740.	810	0.620	1.140	0.5640	55.290
20	1	0.67	70.	0.5	0.098	5330.	6770.	1045	0.152	0.811	0.1470	40.285
21	1	0.63	91.	0.5	0.098	5230.	5230.	131	0.418	0.792	0.5273	49.390
22	1	0.74	100.	0.5	0.098	1840.	1980.	12	0.129	0.220	0.0936	32.432
23	1	0.72	78.	0.5	0.098	2750.	4300.	3410	0.073	0.437	0.1606	27.242
24	1	0.66	76.	1.0	0.387	4920.	4210.	10	0.343	0.502	0.6427	64.592
25	1	0.74	61.	0.5	0.094	6240.	6240.	969	0.522	0.766	0.8821	45.496
41	1	0.67	88.	0.5	0.115	8940.	8940.	83	VAR	0.395	0.0000	VAR
43	1	0.65	61.	0.5	0.126	11840.	10340.	97	VAR	1.004	0.0000	VAR
45	1	0.69	56.	1.0	0.115	12430.	10640.	88	VAR	1.262	0.0000	VAR
48	1	0.67	60.	0.5	0.098	9230.	9230.	74	VAR	1.000	0.0000	VAR
48	2	0.67	63.	1.0	0.088	11750.	9660.	52	VAR	1.215	0.0000	VAR
50	0	0.68	59.	0.5	0.088	7240.	6320.	133	VAR	0.857	0.0000	VAR

VICKSBURG LOESS  
NUMBER OF TESTS = 9  
PERCENT PASSING NO. 200 SIEVE = 98.  
PLASTICITY INDEX = 0.  
LIQUID LIMIT = 29.

TEST NO.	RECORD NO.	VOID RATIO	PERCENT SATURATION	CHAMBER PRESSURE KG/SQ CM	PRINCIPAL STRESS DIFFERENCE KG/SQ CM	INITIAL MAX G PSI	RECOVERY MAX G PSI	CYCLES OFF/RECOVERY	SHEAR STRESS INCREMENT KG/SQ CM	MAXIMUM SHEAR STRESS KG/SQ CM	SHEAR STRESS RATIO	LOAD RATE KG/SQ CM PER HOUR
(11)	(12)	(13)	(14)	(15)	(16)	(17)	(18)	(19)	(20)	(21)	(22)	(23)
26	1	0.67	75.	0.7	0.072	9400.	7400.	1968	0.208	0.755	0.2755	34.224
27	1	0.67	73.	1.4	0.077	12130.	13800.	1155	0.504	1.280	0.3934	47.684
28	1	0.66	66.	2.1	0.062	14130.	22500.	1313	0.550	1.930	0.2891	46.751
29	1	0.65	73.	2.8	0.046	16830.	17450.	5300	0.561	2.250	0.2493	454.229
30	1	0.64	81.	0.7	0.094	8460.	8730.	2256	0.103	0.640	0.1224	77.768
31	1	0.64	83.	0.7	0.094	11590.	11590.	1195	0.368	0.835	0.6572	36.238
32	1	0.64	76.	1.4	0.076	10030.	16720.	6355	0.314	1.370	0.2790	74.132
33	1	0.66	76.	2.1	0.064	16720.	16720.	2770	0.310	1.774	0.1780	73.408
42	1	0.68	76.	0.5	0.096	9630.	9630.	94	VAR	0.793	0.0000	VAR

Table 3. Data for Simple Shear Tests of Low Plasticity Soils (cont').

KENTUCKY													
NUMBER OF TESTS = 4													
PERCENT PASSING NO. 200 SIEVE = 94.													
PLASTICITY INDEX = 11.													
LIQUID LIMIT = 40.													
TEST NO.	RECORD NO.	VOID RATIO	PERCENT SATURATION	CHAMBER PRESSURE KG/50 CM	PRINCIPAL STRESS DIFFERENCE KG/50 CM	INITIAL MAX. σ PSI	RECOVERY MAX. σ PSI	CYCLES BEFORE RECOVERY	SHEAR STRESS INCREMENT KG/50 CM	MAXIMUM SHEAR STRESS KG/50 CM	SHEAR STRESS RATIO	LOAD RATE KG/50 CM PER HOUR	
64	1	0.57	66.	0.5	101	171	181	191	1101	1111	1121	1131	
65	1	0.57	67.	0.7	0.094	1200.	1410.	980	0.379	0.801	0.6397	40.808	
66	1	0.59	71.	1.4	0.094	1340.	1550.	880	0.490	0.945	0.6976	40.765	
67	1	0.63	78.	2.5	0.098	1620.	1920.	7800	0.591	0.945	0.6258	40.765	
ALLEN													
NUMBER OF TESTS = 4													
PERCENT PASSING NO. 200 SIEVE = 39.													
PLASTICITY INDEX = 9.													
LIQUID LIMIT = 30.													
TEST NO.	RECORD NO.	VOID RATIO	PERCENT SATURATION	CHAMBER PRESSURE KG/50 CM	PRINCIPAL STRESS DIFFERENCE KG/50 CM	INITIAL MAX. σ PSI	RECOVERY MAX. σ PSI	CYCLES BEFORE RECOVERY	SHEAR STRESS INCREMENT KG/50 CM	MAXIMUM SHEAR STRESS KG/50 CM	SHEAR STRESS RATIO	LOAD RATE KG/50 CM PER HOUR	
81	1	0.69	64.	0.5	101	171	181	191	1101	1111	1121	1131	
82	1	0.58	64.	0.5	0.094	1100.	1260.	200	0.432	0.637	0.6782	40.916	
84	1	0.70	51.	1.0	0.088	920.	920.	1	0.433	0.504	0.5593	41.318	
85	1	0.68	75.	1.5	0.076	1320.	2310.	1825	0.210	0.967	0.2169	41.305	
KENTUCKY SS													
NUMBER OF TESTS = 2													
PERCENT PASSING NO. 200 SIEVE = 60.													
PLASTICITY INDEX = 9.													
LIQUID LIMIT = 36.													
TEST NO.	RECORD NO.	VOID RATIO	PERCENT SATURATION	CHAMBER PRESSURE KG/50 CM	PRINCIPAL STRESS DIFFERENCE KG/50 CM	INITIAL MAX. σ PSI	RECOVERY MAX. σ PSI	CYCLES BEFORE RECOVERY	SHEAR STRESS INCREMENT KG/50 CM	MAXIMUM SHEAR STRESS KG/50 CM	SHEAR STRESS RATIO	LOAD RATE KG/50 CM PER HOUR	
86	1	0.58	99.	0.5	0.098	710.	710.	2533	0.223	1.020	0.2190	38.881	
90	1	0.60	100.	0.5	0.098	600.	933.	1274	0.221	0.633	0.3494	7.794	
LONGHORN													
NUMBER OF TESTS = 4													
PERCENT PASSING NO. 200 SIEVE = 46.													
PLASTICITY INDEX = 13.													
LIQUID LIMIT = 29.													
TEST NO.	RECORD NO.	VOID RATIO	PERCENT SATURATION	CHAMBER PRESSURE KG/50 CM	PRINCIPAL STRESS DIFFERENCE KG/50 CM	INITIAL MAX. σ PSI	RECOVERY MAX. σ PSI	CYCLES BEFORE RECOVERY	SHEAR STRESS INCREMENT KG/50 CM	MAXIMUM SHEAR STRESS KG/50 CM	SHEAR STRESS RATIO	LOAD RATE KG/50 CM PER HOUR	
91	1	0.65	74.	0.5	101	171	181	191	1101	1111	1121	1131	
92	1	0.61	81.	1.0	0.094	1220.	1370.	5317	0.212	0.691	0.3065	36.073	
93	1	0.63	70.	1.5	0.088	1040.	1350.	1235	0.288	1.312	0.2140	36.430	
94	1	0.64	70.	0.5	0.076	1030.	1940.	1047	0.530	1.731	0.3064	40.479	
WEST VIRGINIA SHALE													
NUMBER OF TESTS = 4													
PERCENT PASSING NO. 200 SIEVE = 85.													
PLASTICITY INDEX = 4.													
LIQUID LIMIT = 25.													
TEST NO.	RECORD NO.	VOID RATIO	PERCENT SATURATION	CHAMBER PRESSURE KG/50 CM	PRINCIPAL STRESS DIFFERENCE KG/50 CM	INITIAL MAX. σ PSI	RECOVERY MAX. σ PSI	CYCLES BEFORE RECOVERY	SHEAR STRESS INCREMENT KG/50 CM	MAXIMUM SHEAR STRESS KG/50 CM	SHEAR STRESS RATIO	LOAD RATE KG/50 CM PER HOUR	
95	1	0.61	64.	0.5	101	171	181	191	1101	1111	1121	1131	
96	1	0.62	64.	1.0	0.094	980.	1020.	1883	0.358	0.847	0.4228	31.726	
97	1	0.61	68.	1.5	0.076	1370.	1950.	1787	0.615	1.110	0.5545	30.424	
98	1	0.38	92.	1.0	0.088	1310.	1800.	596	0.614	1.518	0.4075	30.570	
VIRGINIA CLAY													
NUMBER OF TESTS = 4													
PERCENT PASSING NO. 200 SIEVE = 98.													
PLASTICITY INDEX = 22.													
LIQUID LIMIT = 66.													
TEST NO.	RECORD NO.	VOID RATIO	PERCENT SATURATION	CHAMBER PRESSURE KG/50 CM	PRINCIPAL STRESS DIFFERENCE KG/50 CM	INITIAL MAX. σ PSI	RECOVERY MAX. σ PSI	CYCLES BEFORE RECOVERY	SHEAR STRESS INCREMENT KG/50 CM	MAXIMUM SHEAR STRESS KG/50 CM	SHEAR STRESS RATIO	LOAD RATE KG/50 CM PER HOUR	
119	1	0.77	94.	1.0	101	171	181	191	1101	1111	1121	1131	
120	1	0.60	73.	0.5	0.087	1120.	1170.	1524	0.428	1.073	0.3987	60.053	
21	1	0.62	40.	1.5	0.077	1600.	1650.	2301	0.211	1.096	0.1926	32.563	
26	1	0.78	65.	2.0	0.076	1600.	2050.	203	0.214	1.920	0.1114	1.629	

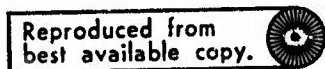


Table 4. Data for Simple Shear Tests of High Plasticity Soils.

ILLINOIS CLAY NUMBER OF TESTS = 5 PERCENT PASSING NO. 200 SIEVE = 91. PLASTICITY INDEX = 32. LIQUID LIMIT = 66.												
TEST NO.	RECORD NO.	VOID RATIO	PERCENT SATURATION	CHAMBER PRESSURE KG/SQ CM	PRINCIPAL STRESS DIFFERENCE KG/SQ CM	INITIAL MAX G PSI	RECOVERY MAX G PSI	CYCLES BEFORE RECOVERY	SHEAR STRESS INCREMENT KG/SQ CM	MAXIMUM SHEAR STRESS KG/SQ CM	SHEAR STRESS RATIO	LOAD RATE KG/SQ CM PER HOUR
(1)	(2)	(3)	(4)	(5)	(6)	(7)	(8)	(9)	(10)	(11)	(12)	(13)
51	1	0.67	66.	0.5	0.096	2210.	9600.	330	0.205	1.006	0.2042	42.378
52	1	0.68	66.	1.0	0.088	10030.	10900.	785	0.581	1.344	0.4322	35.811
53	1	0.84	35.	3.5	0.098	10310.	10800.	1174	0.425	1.086	0.3910	39.916
55	1	0.61	72.	1.0	0.088	11760.	13560.	299	0.534	1.891	0.2823	12.075
78	1	0.88	92.	0.5	0.096	2300.	5860.	6926	0.100	0.355	0.2805	21.199
CHIEKS NUMBER OF TESTS = 4 PERCENT PASSING NO. 200 SIEVE = 82. PLASTICITY INDEX = 36. LIQUID LIMIT = 66.												
TEST NO.	RECORD NO.	VOID RATIO	PERCENT SATURATION	CHAMBER PRESSURE KG/SQ CM	PRINCIPAL STRESS DIFFERENCE KG/SQ CM	INITIAL MAX G PSI	RECOVERY MAX G PSI	CYCLES BEFORE RECOVERY	SHEAR STRESS INCREMENT KG/SQ CM	MAXIMUM SHEAR STRESS KG/SQ CM	SHEAR STRESS RATIO	LOAD RATE KG/SQ CM PER HOUR
(1)	(2)	(3)	(4)	(5)	(6)	(7)	(8)	(9)	(10)	(11)	(12)	(13)
60	1	1.20	97.	0.5	0.098	12730.	17890.	1111	0.314	1.180	0.2657	10.382
61	1	1.15	61.	0.5	0.098	12.30.	12230.	614	0.564	1.083	0.5204	38.196
62	1	1.14	60.	1.0	0.088	14510.	17140.	403	0.570	1.554	0.3671	34.604
63	1	0.99	98.	0.5	0.098	9790.	12450.	1160	0.353	0.636	0.5536	38.673
NEVADA CLAY NUMBER OF TESTS = 4 PERCENT PASSING NO. 200 SIEVE = 100. PLASTICITY INDEX = 52. LIQUID LIMIT = 93.												
TEST NO.	RECORD NO.	VOID RATIO	PERCENT SATURATION	CHAMBER PRESSURE KG/SQ CM	PRINCIPAL STRESS DIFFERENCE KG/SQ CM	INITIAL MAX G PSI	RECOVERY MAX G PSI	CYCLES BEFORE RECOVERY	SHEAR STRESS INCREMENT KG/SQ CM	MAXIMUM SHEAR STRESS KG/SQ CM	SHEAR STRESS RATIO	LOAD RATE KG/SQ CM PER HOUR
(1)	(2)	(3)	(4)	(5)	(6)	(7)	(8)	(9)	(10)	(11)	(12)	(13)
68	1	1.38	82.	0.5	0.098	7750.	9800.	2209	0.214	0.966	0.2268	40.424
69	1	1.42	82.	1.0	0.088	7670.	9180.	940	0.479	1.172	0.4089	40.913
70	1	1.45	99.	0.5	0.098	4940.	5690.	1357	0.365	0.727	0.5020	39.655
71	1	1.39	97.	1.0	0.088	6000.	7700.	5177	0.346	0.905	0.3824	36.965
LOUISIANA CLAY NUMBER OF TESTS = 1 PERCENT PASSING NO. 200 SIEVE = 98. PLASTICITY INDEX = 30. LIQUID LIMIT = 61.												
TEST NO.	RECORD NO.	VOID RATIO	PERCENT SATURATION	CHAMBER PRESSURE KG/SQ CM	PRINCIPAL STRESS DIFFERENCE KG/SQ CM	INITIAL MAX G PSI	RECOVERY MAX G PSI	CYCLES BEFORE RECOVERY	SHEAR STRESS INCREMENT KG/SQ CM	MAXIMUM SHEAR STRESS KG/SQ CM	SHEAR STRESS RATIO	LOAD RATE KG/SQ CM PER HOUR
(1)	(2)	(3)	(4)	(5)	(6)	(7)	(8)	(9)	(10)	(11)	(12)	(13)
125	1	1.12	100.	0.8	0.087	1350.	2980.	324	0.130	0.483	0.2609	1.120
SAN FRANCISCO CLAY NUMBER OF TESTS = 3 PERCENT PASSING NO. 200 SIEVE = 99. PLASTICITY INDEX = 35. LIQUID LIMIT = 62.												
TEST NO.	RECORD NO.	VOID RATIO	PERCENT SATURATION	CHAMBER PRESSURE KG/SQ CM	PRINCIPAL STRESS DIFFERENCE KG/SQ CM	INITIAL MAX G PSI	RECOVERY MAX G PSI	CYCLES BEFORE RECOVERY	SHEAR STRESS INCREMENT KG/SQ CM	MAXIMUM SHEAR STRESS KG/SQ CM	SHEAR STRESS RATIO	LOAD RATE KG/SQ CM PER HOUR
(1)	(2)	(3)	(4)	(5)	(6)	(7)	(8)	(9)	(10)	(11)	(12)	(13)
127	1	1.01	100.	1.0	0.087	2770.	4310.	2168	0.105	0.637	0.1641	17.142
129	1	0.91	100.	1.5	0.087	4080.	5407.	513	0.135	0.823	0.1642	1.265
130	1	0.85	100.	2.5	0.087	4800.	6643.	476	0.213	1.067	0.1997	7.759

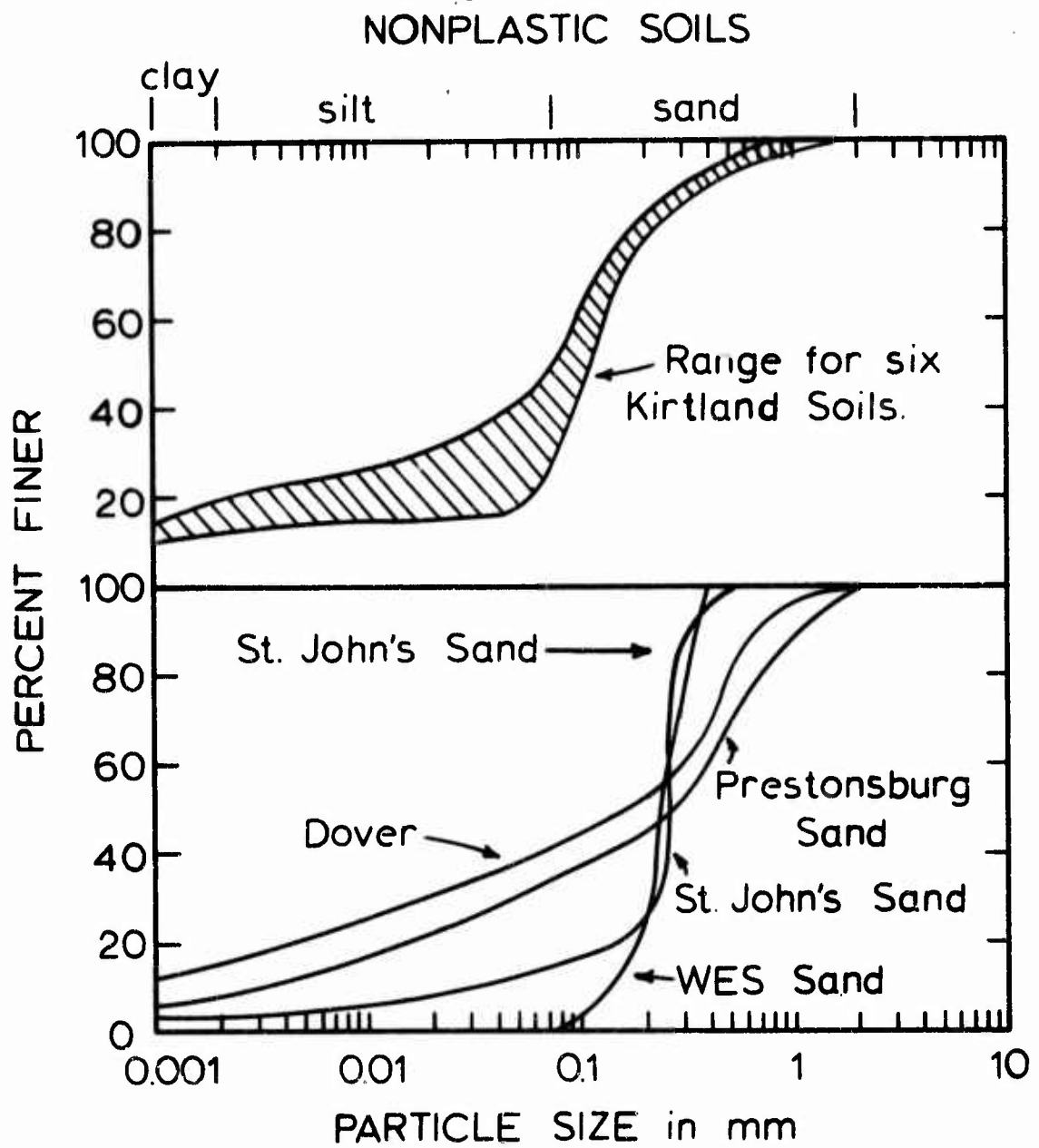


Figure 10. Particle size distribution curves for nonplastic soils.

## LOW PLASTICITY SOILS

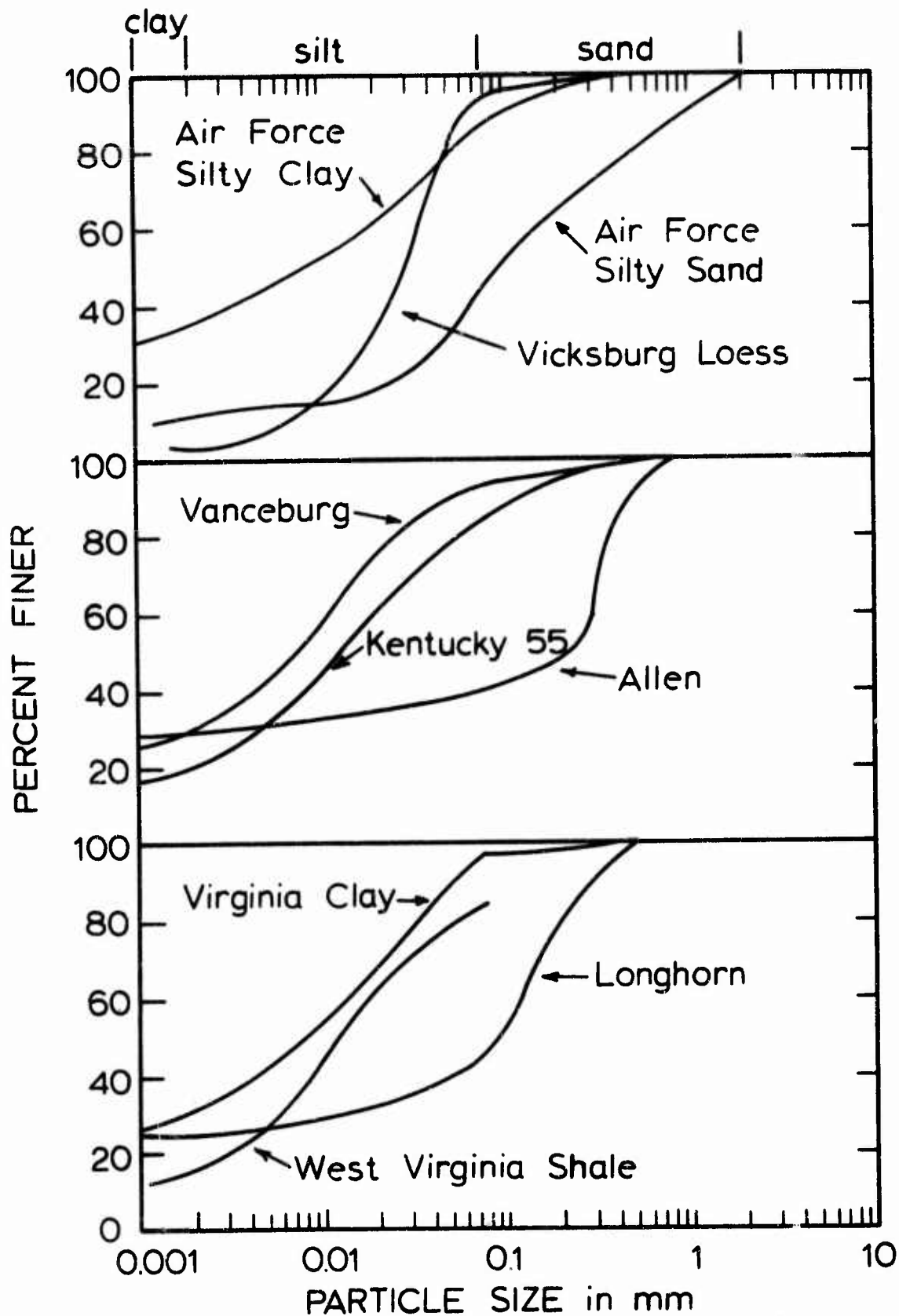


Figure 11. Particle size distribution curves for low plasticity soils.

## HIGH PLASTICITY SOILS

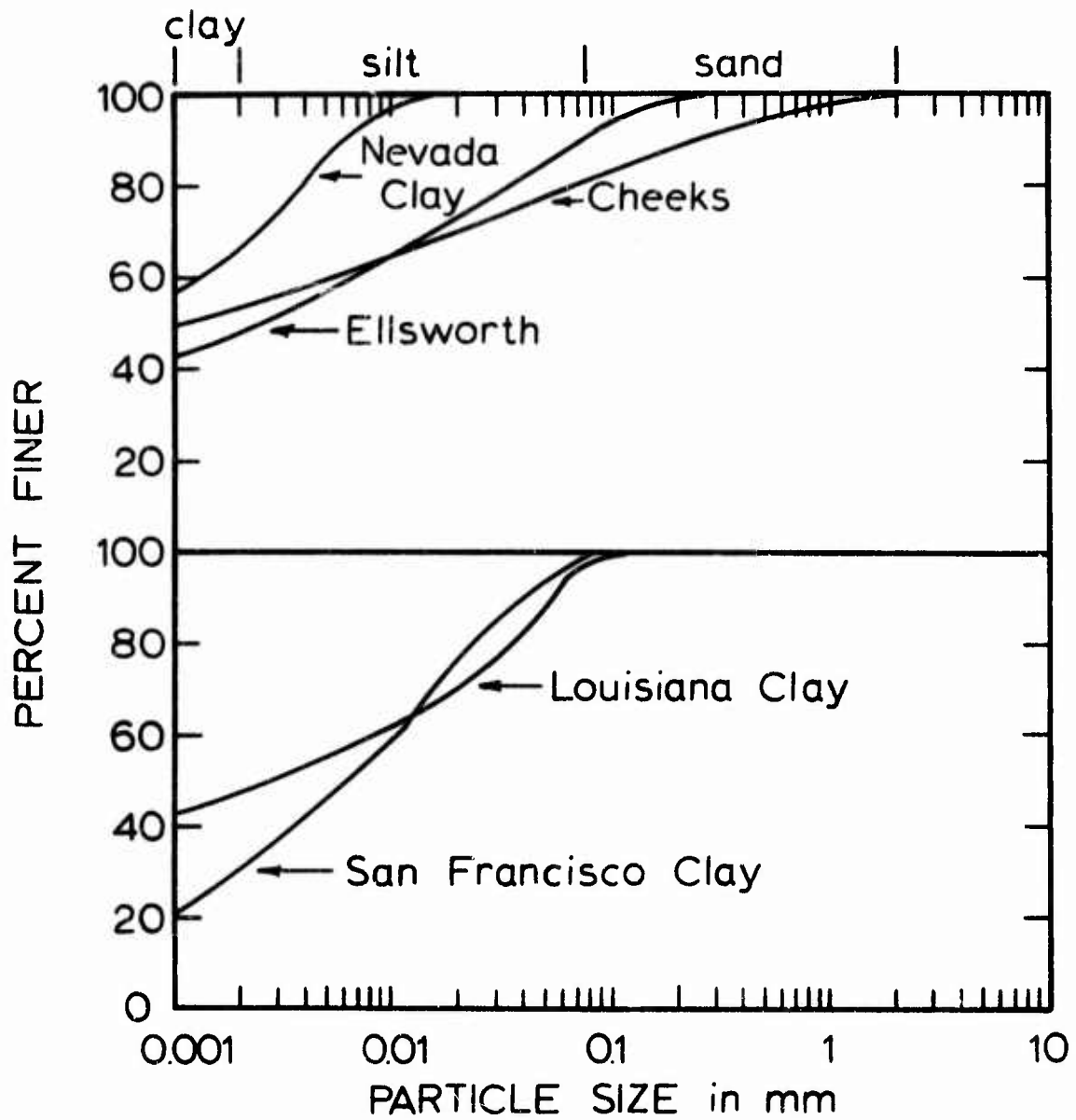


Figure 12. Particle size distribution curves for high plasticity soils.

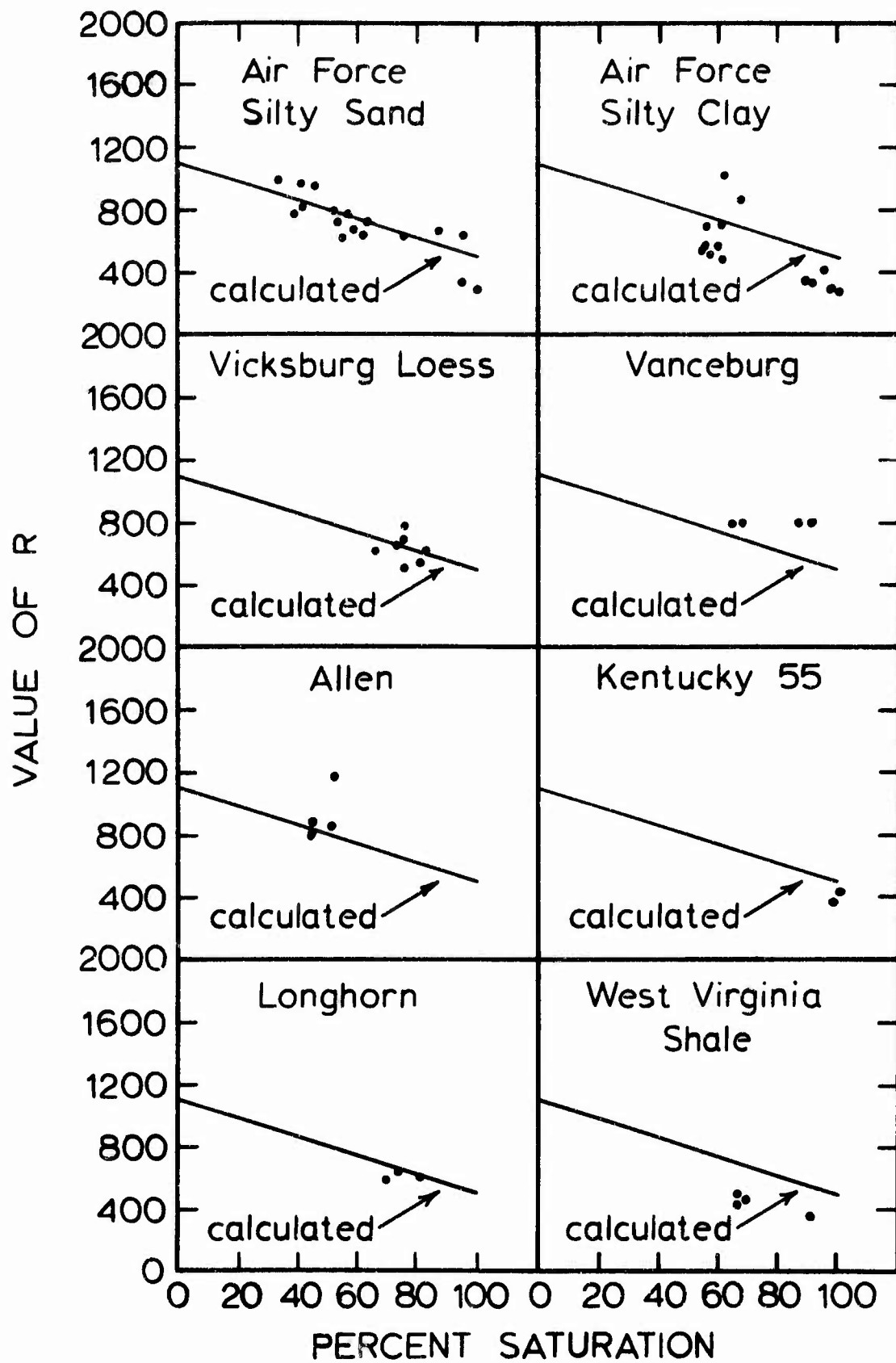


Figure 13. Comparison of the variation of experimental and calculated values of R with percent saturation, Air Force Silty Sand, Air Force Silty Clay, Vicksburg Loess, Vanceburg, Allen, Kentucky 55, Longhorn, and West Virginia Shale.

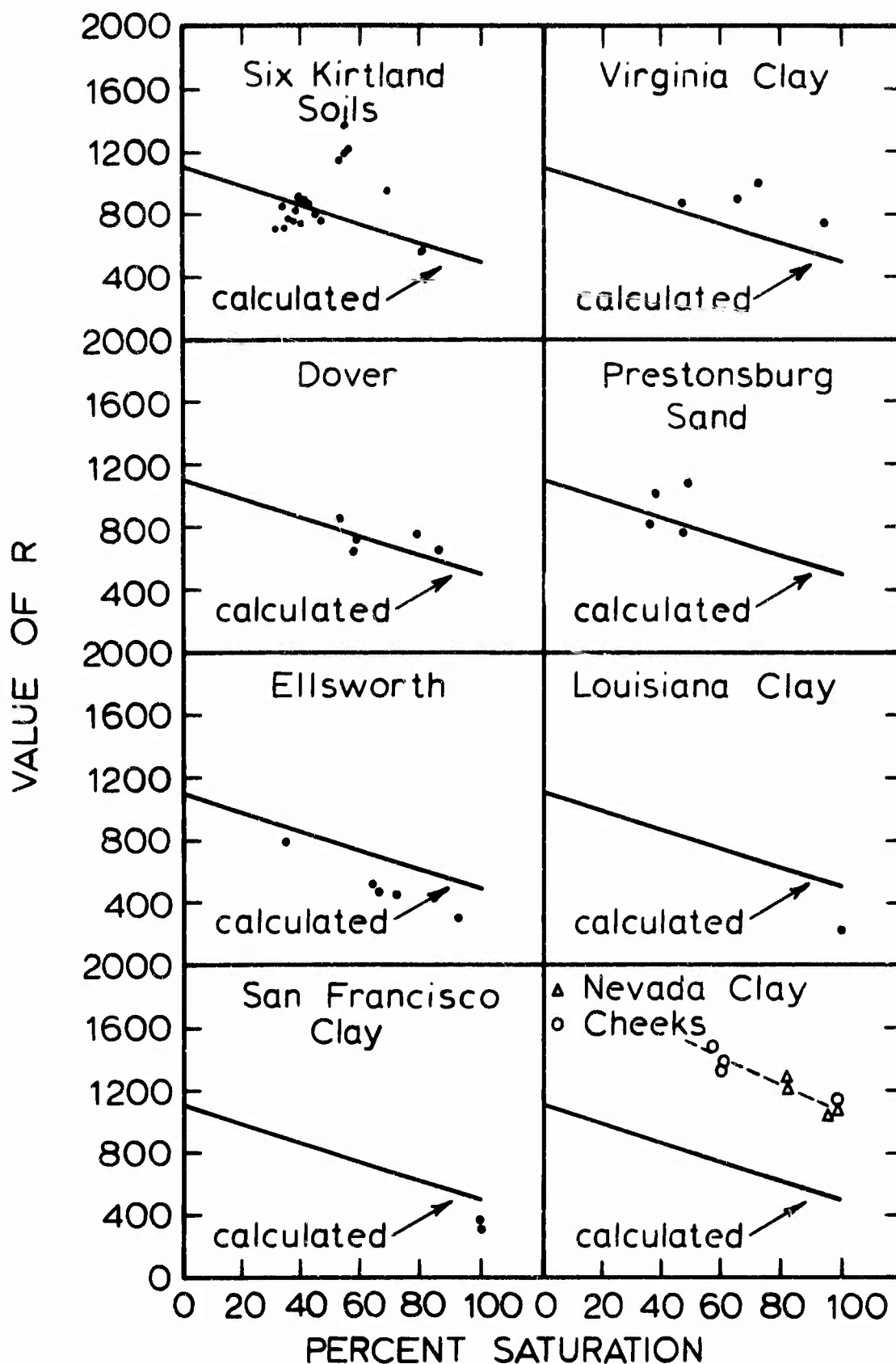


Figure 14. Comparison of the variation of experimental and calculated values of R with percent saturation, Six Kirtland Soils, Virginia Clay, Dover, Prestonsburg Sand, Ellsworth, Louisiana Clay, San Francisco Clay, Cheeks, and Nevada Clay.

experimental values. The weakest comparison is with two of the high plasticity soils, the Cheeks and Nevada Clays. Here the measured and calculated values differ by a factor of 2. However, the Louisiana and San Francisco Clays are also high plasticity soils, and they more nearly conform to the pattern of the other cohesive soils than to the Cheeks and Nevada Clays. Hence, the use of equation 3 for high plasticity soils is rather uncertain but is the best available at present.

The measured values of R for sands with less than 15 percent fines are shown in table 5. The average value from 10 tests of dry WES sand is 1102 with about 10 percent scatter. The average value for the St. John's Sand with tests at both 88 and 100 percents saturation is 1224, with the value for test no. 76 being excessively high. The average for the St. John's Sand excluding test no. 76 is 1104, which nearly equals the value for the dry sand. From this it was concluded that for sands with less than 15 percent fines  $R = 1100$  could be used for all percents saturation, as shown by the first of equation 3.

The value of R defines the relationship between  $\tau_{\max}$  and  $G_{\max}$ . As shown in Appendix I, equation 11 can be rearranged to eliminate  $\tau_{\max}$  for reference strain, and obtain the reference strain in terms of  $G_{\max}$  as given by equation 1. Therefore, the data in figures 13 and 14 and in table 5 defining the value of R, are the basis for the equations given in Section II, paragraph 2 for determination of the reference strain, and indicate the degree of accuracy that may be expected when using that part of the practical procedure.

Table 5. Values of R for Sands with Less than 15 Percent Fines.

WES Sand (dry)		St. John's Sand		
Test No.	Value of R	Test No.	Percent Saturation	Value of R
34	1045	76	100	1584
35	1094	77	100	1313
36	1046	79	88	1064
37	1026	80	88	934
38	1101			
39	1116			
83	990			
89	1167			
101	1125			
112	1311			
Avg.	1102			1224

### 3. Comparison of Shear Modulus Values

The variations of normalized shear modulus with normalized strain, as given by equations 8 and 9, are shown in figure 15 for different values of  $a$ . When  $a = 0$  the relationship is hyperbolic. Figure 15 shows that higher values of  $a$  give lower values of  $G/G_{\max}$  for a given  $\gamma/\gamma_r$ . Using measured values for  $G$ ,  $G_{\max}$ ,  $\tau_{\max}$ , and  $\gamma$ , experimental values of the normalized shear modulus and normalized strain can be calculated. In figures 16 through 22 such experimental values are compared to the values given by equations 8, 9, and 10 of the practical procedure. Figures 16 through 22 are for the first cycle of loading. One test of each different soil was chosen to show the comparison. The tests shown were not chosen because they gave the best comparisons. The parameters necessary for obtaining the calculated curve from equations 8, 9, and 10 are shown in the upper right hand corner of each graph. The shapes of the calculated curves correspond to various values of  $a$  between 0.33 and 5.34. The accuracy of the practical procedure is quite good considering the range of soil types and conditions to which they are applied.

Comparisons for the 10th and 100th cycles are shown in figures 23 and 24, respectively. For these comparisons the measured value of normalized strain along with the value of  $a$  calculated from equation 10 were used to calculate  $\gamma_h$  from equation 9. This value of  $\gamma_h$  was plotted versus the measured normalized shear modulus, thus locating the different symbols in figures 23 and 24 representing the measured relationship. The calculated relationship shown by the curves in figures 23 and 24 is given by equation 8 and is hyperbolic,

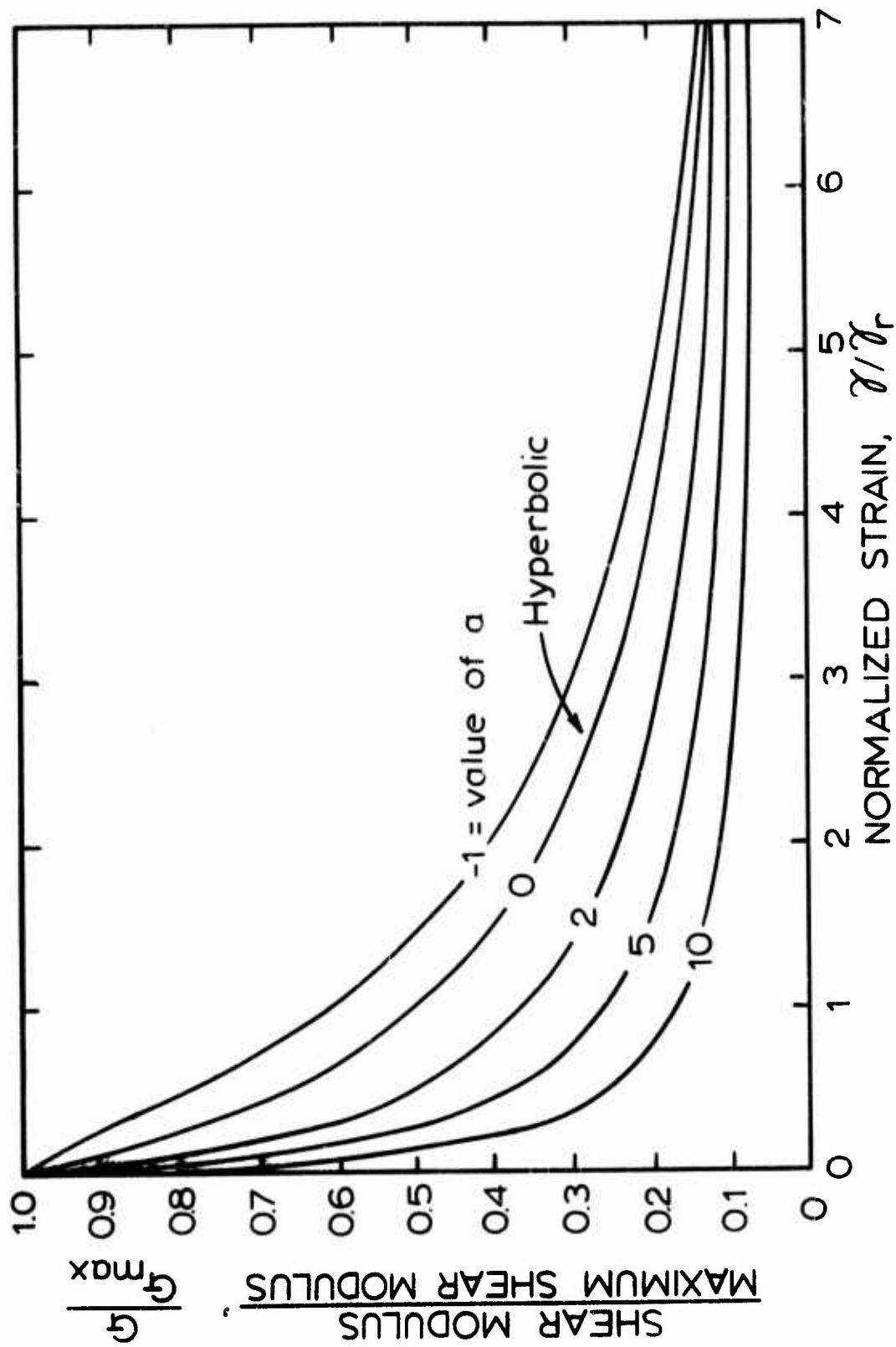


Figure 15. Variation of normalized shear modulus with normalized strain as given by the practical procedure for various values of  $a$ .

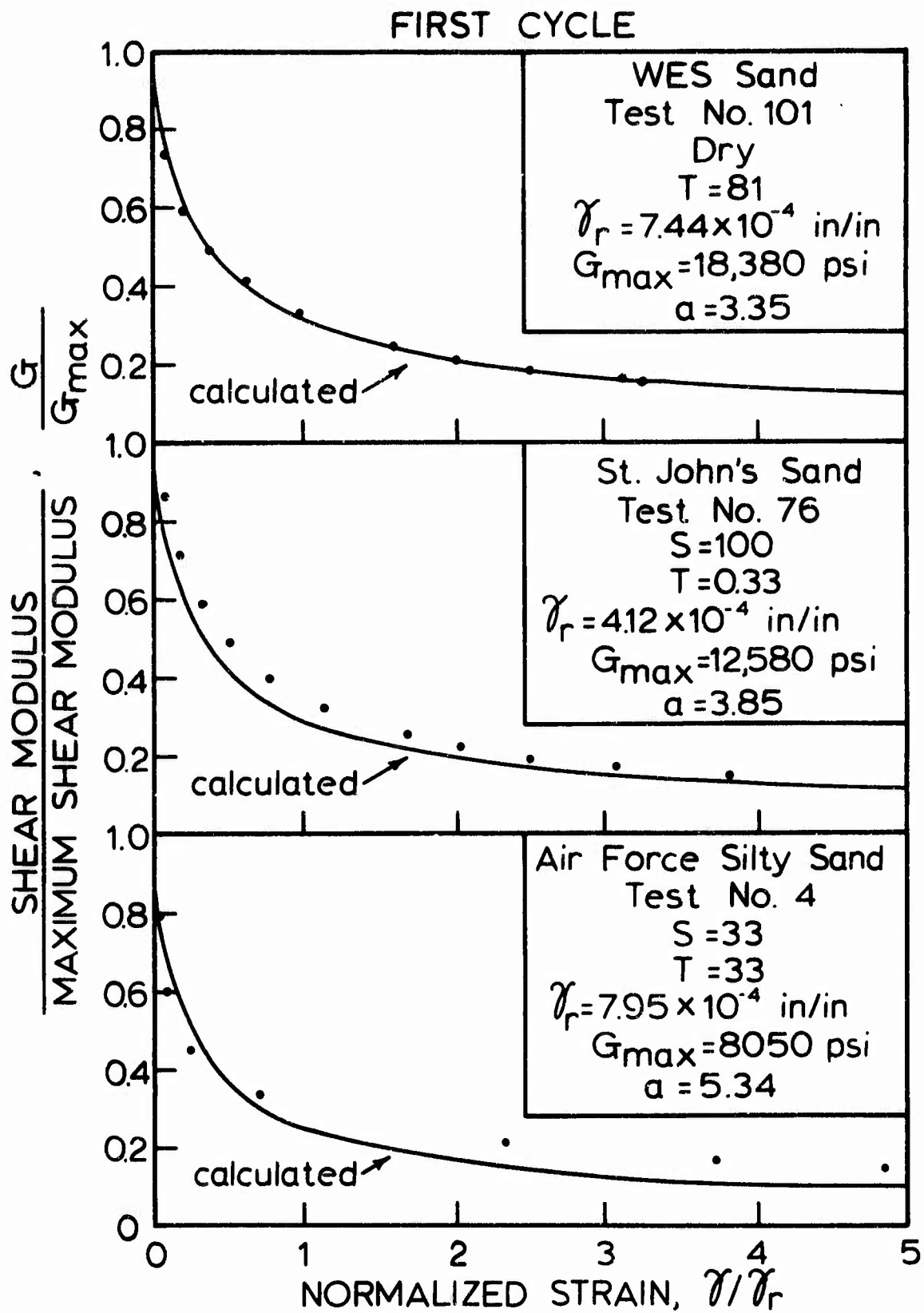


Figure 16. Comparison of measured and calculated values of shear modulus, first cycle, WES Sand, St. John's Sand, and Air Force Silty Sand.

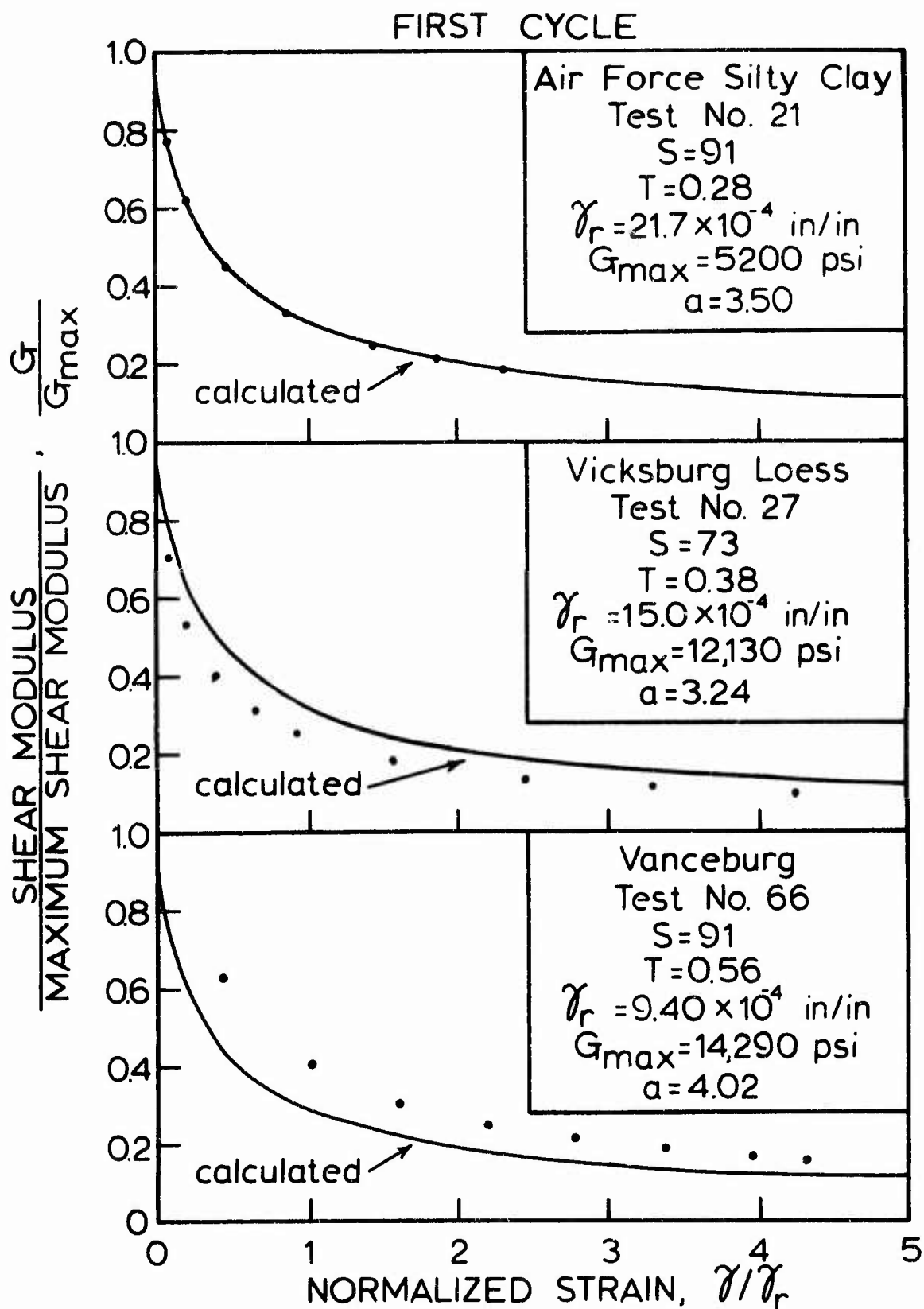


Figure 17. Comparison of measured and calculated values of shear modulus, first cycle, Air Force Silty Clay, Vicksburg Loess, and Vanceburg.

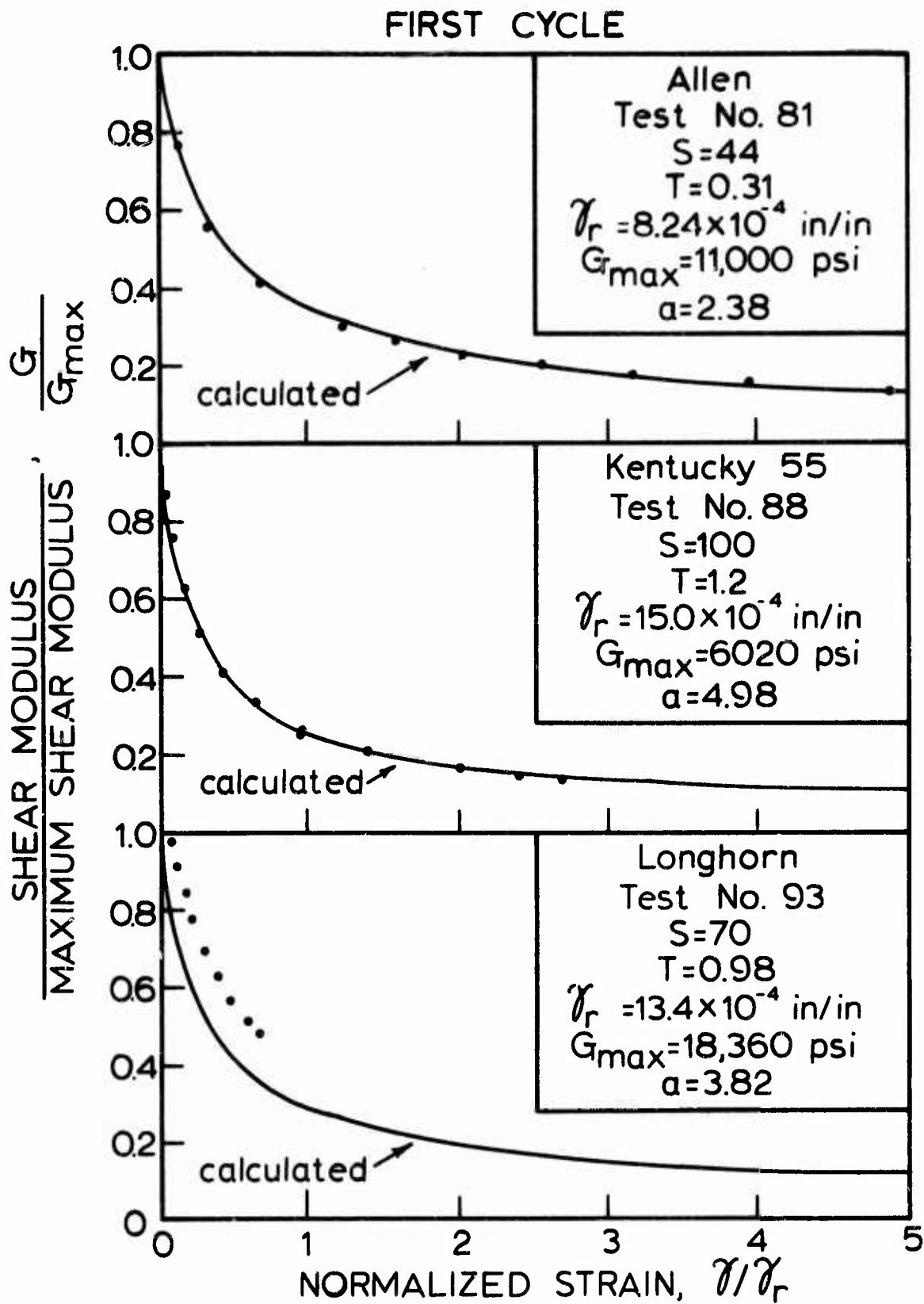


Figure 18. Comparison of measured and calculated values of shear modulus, first cycle, Allen, Kentucky 55, and Longhorn.

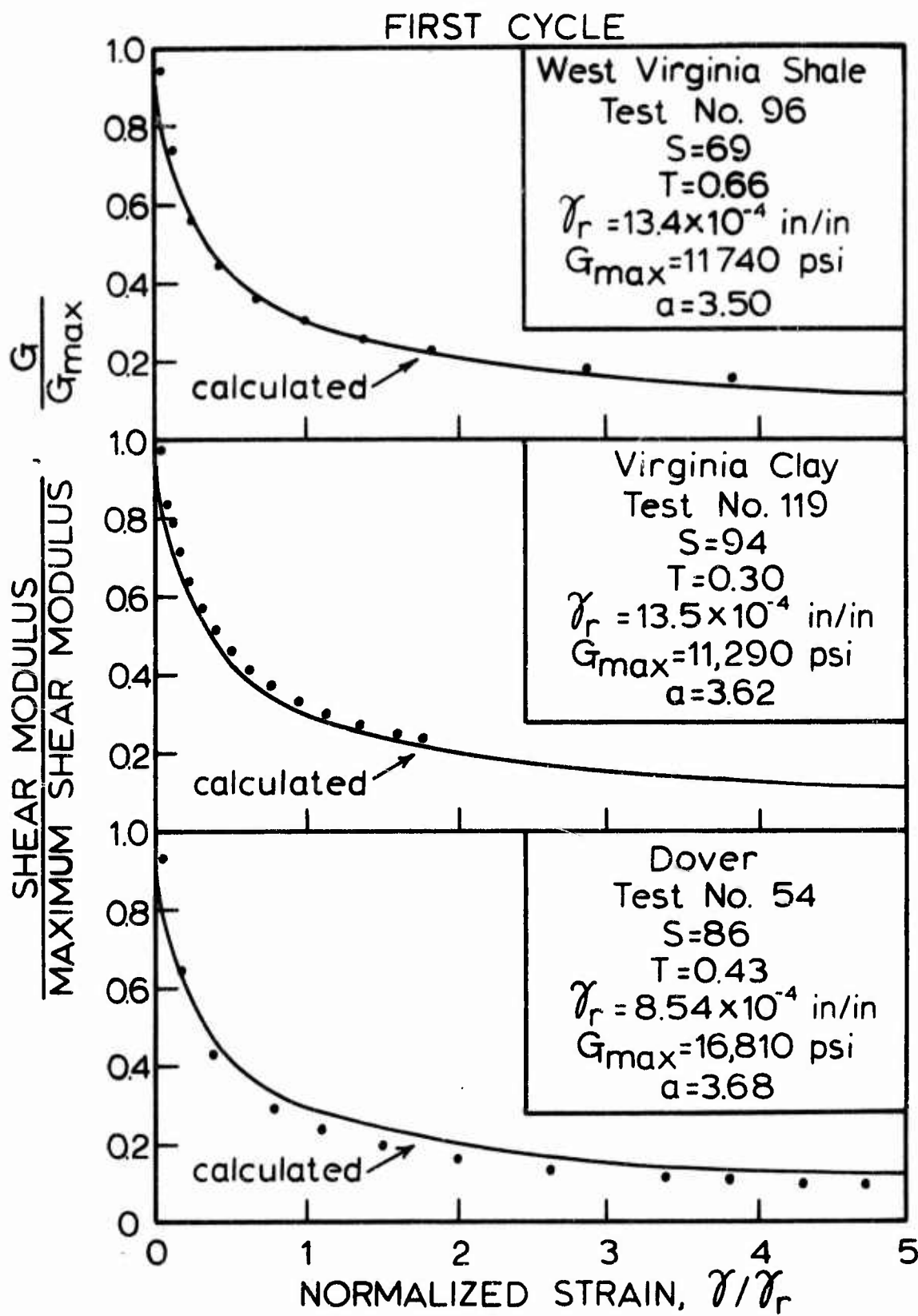


Figure 19. Comparison of measured and calculated values of shear modulus, first cycle, West Virginia Shale, Virginia Clay, and Dover.

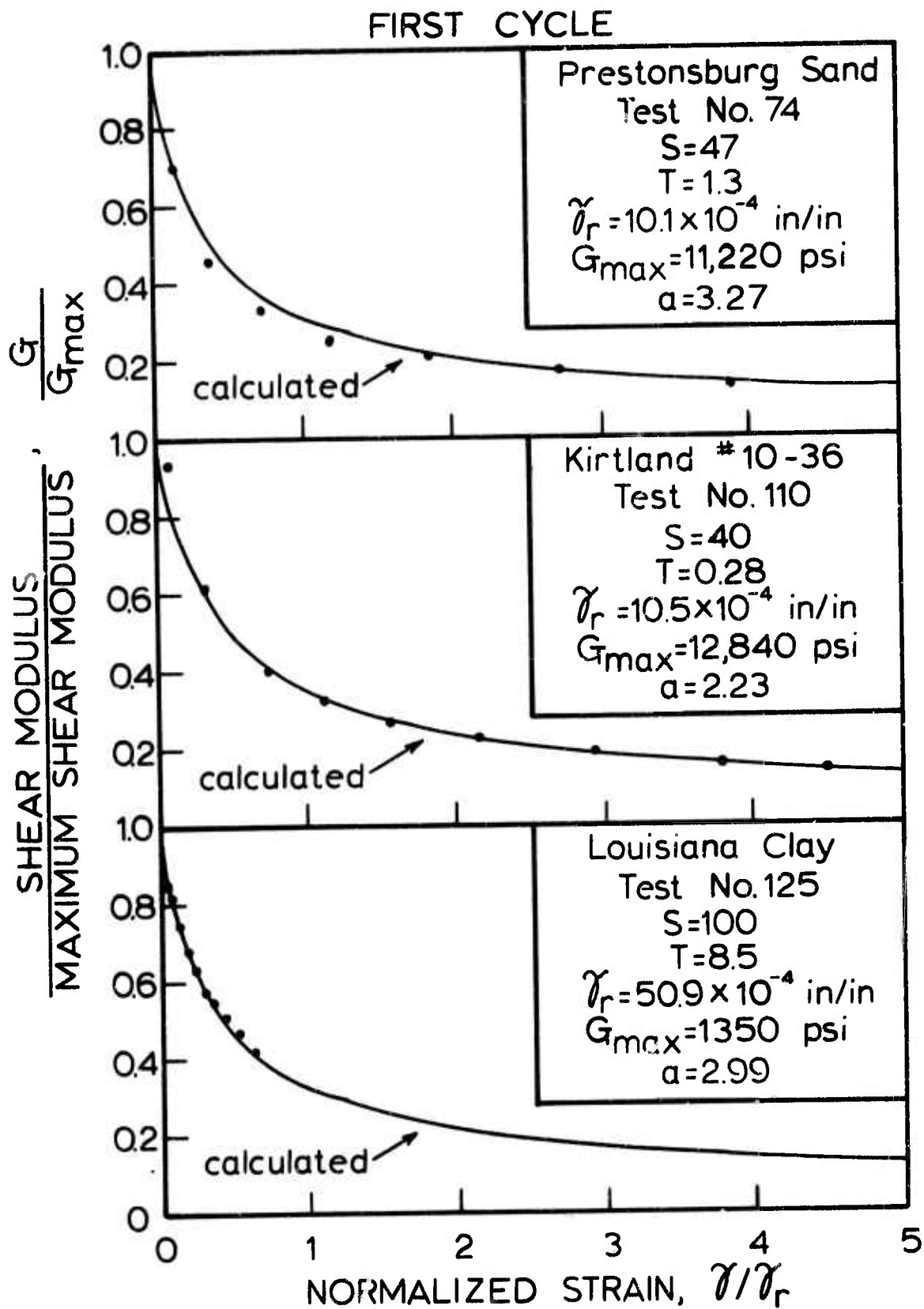


Figure 20. Comparison of measured and calculated values of shear modulus, first cycle, Prestonsburg Sand, Kirtland #10-36, and Louisiana Clay.

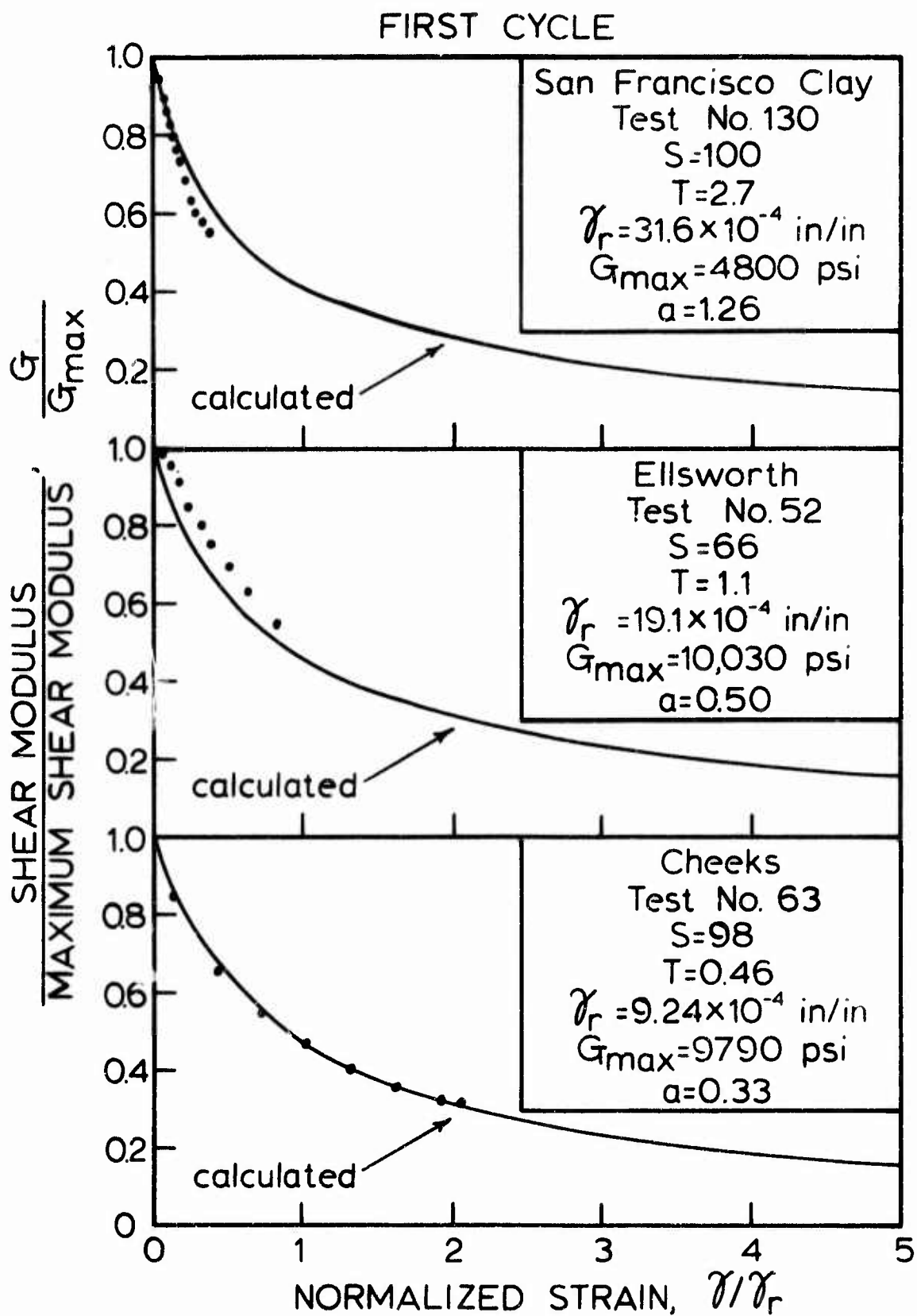


Figure 21. Comparison of measured and calculated values of shear modulus, first cycle, San Francisco Clay, Ellsworth, and Cheeks.

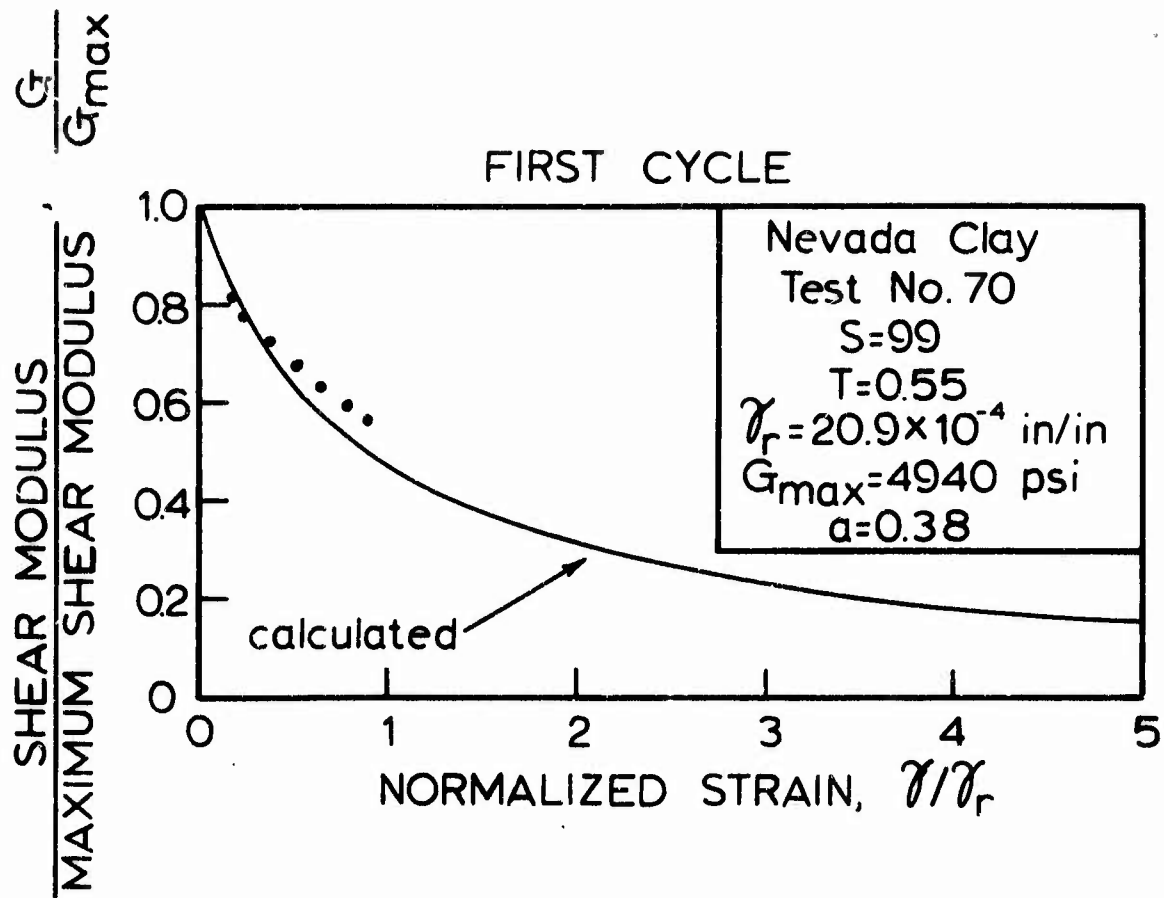


Figure 22. Comparison of measured and calculated values of shear modulus, first cycle, Nevada Clay.

since the hyperbolic strain was used as abscissa. The comparison between measured and calculated values for the 10th and 100th cycles is good.

The hyperbolic strain is used in figures 23 and 24 so that data for different soils with different values of S and T can all be shown on the same graph. When  $G/G_{\max}$  is plotted versus  $\gamma/\gamma_r$ , the expected relationship depends on the values of N, S, T and soil type. A different calculated curve would be needed for each test, as was done in figures 16 through 22 for  $N = 1$ .

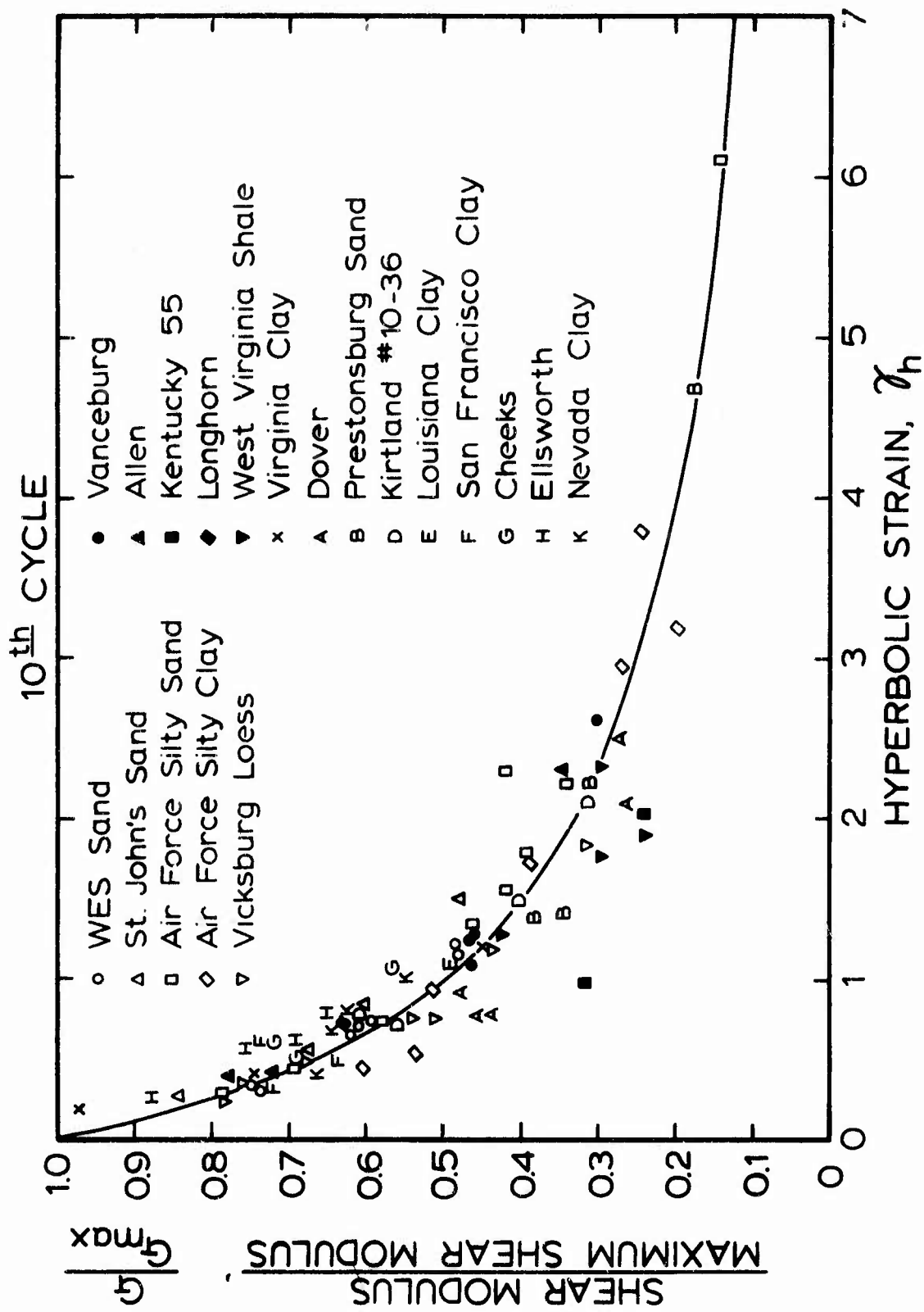


Figure 23. Comparison of measured and calculated values of shear modulus, 10th cycle.

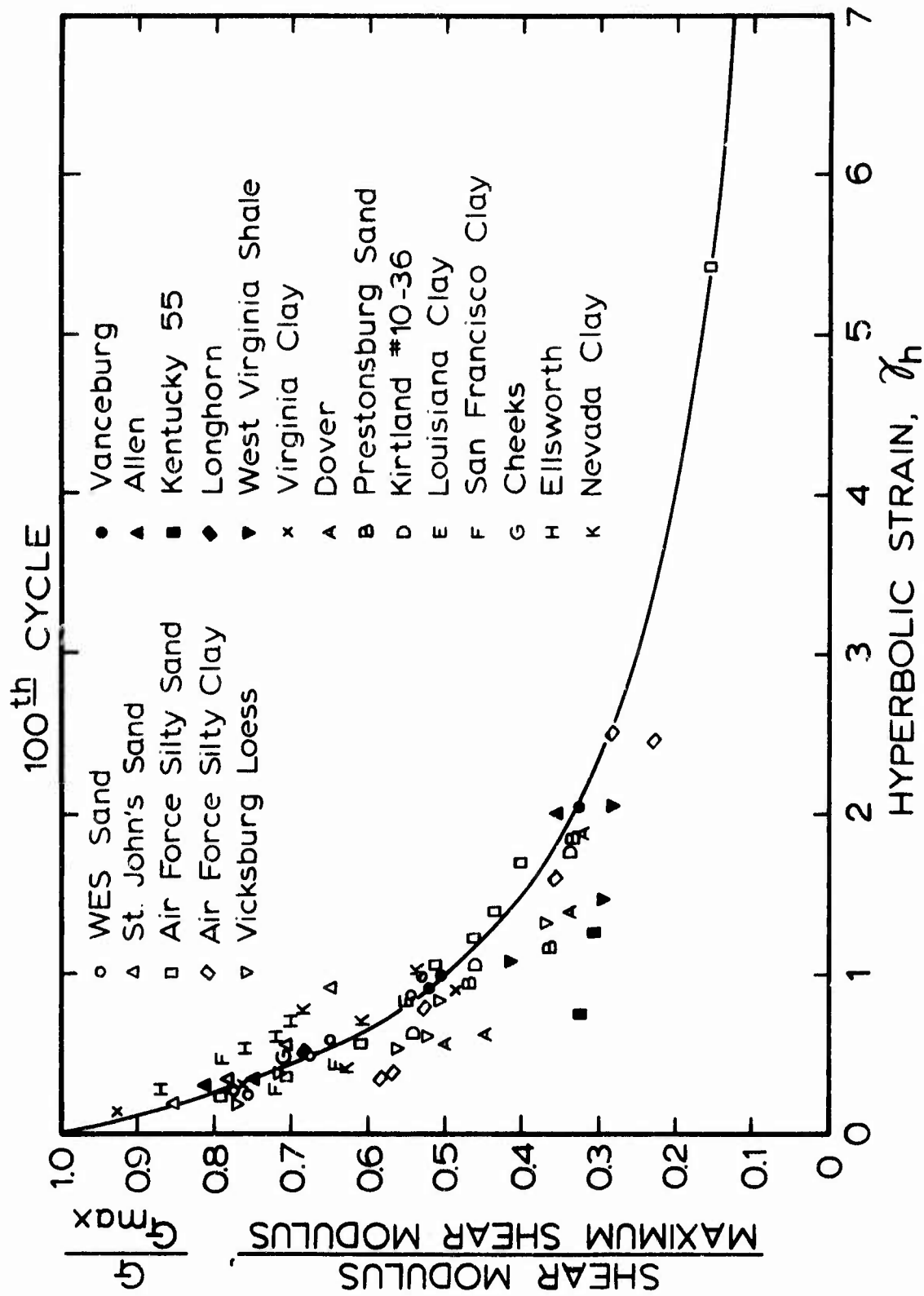


Figure 24. Comparison of measured and calculated values of shear modulus, 100th cycle.

## SECTION IV

### MIXED LOADING AMPLITUDES AND REST PERIODS

#### 1. Objective

For the majority of tests discussed herein a cyclic shear loading was applied continuously, where the next cycle began immediately as the preceding cycle ended, and the loading amplitude was constant for all cycles as was the rate of loading and unloading. Because actual air traffic involves varying length rest periods between load applications and a mixture of light and heavy loadings, it was desirable to assess these effects by conducting tests where the loading could be programmed. Then a soil specimen could be subjected to rest periods, with zero load, between cycles of loading and the amplitude of loading could be different for successive cycles of loading.

#### 2. Loading Programs and Recorded Stress-Strain Relations.

Three primary loading sequences were used for mixed amplitude studies. The first was an increasing load sequence as shown in the top of figure 25. In this figure the ordinate is proportional to the applied shear stress and the abscissa is time. The slope of the lines in this figure are proportional to the rate of loading. The loading program in the top of figure 25 produces a sequence of loads with monotonically increasing amplitudes but with a constant rate of loading and unloading. The second loading sequence shown in the bottom of figure 25 produces a large first load with subsequent loads decreasing in amplitude monotonically. The third sequence was a combination of these two where the sample was subjected first to the increasing load sequence followed by the

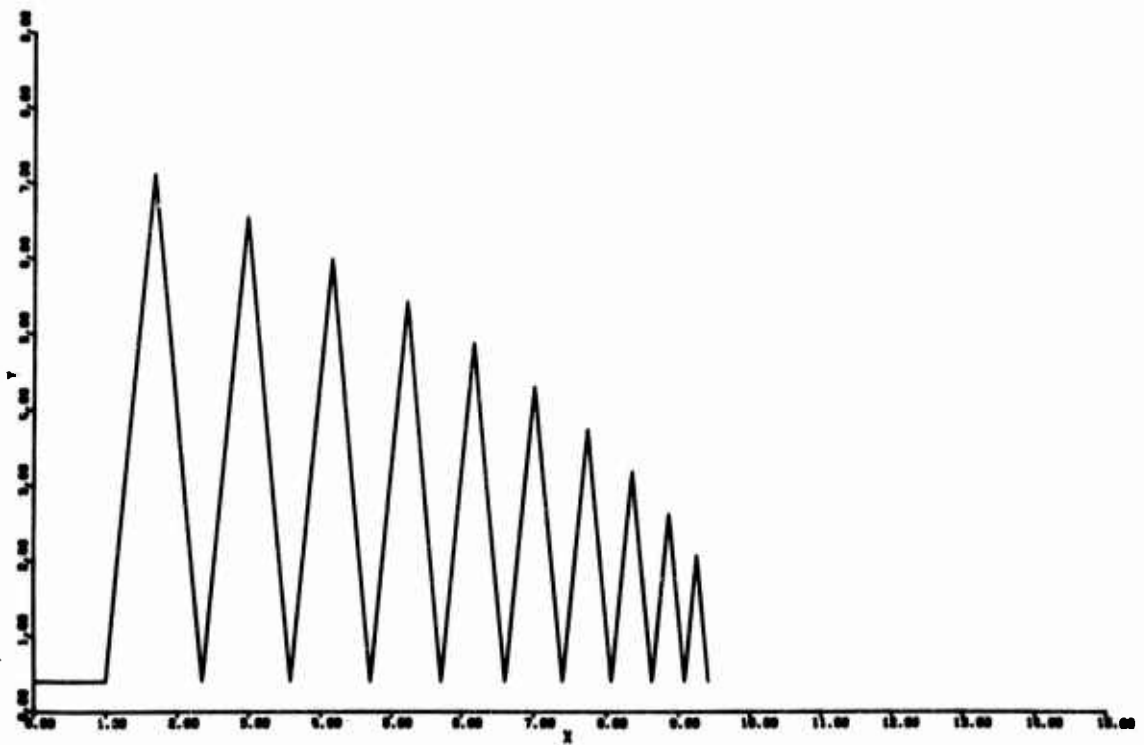
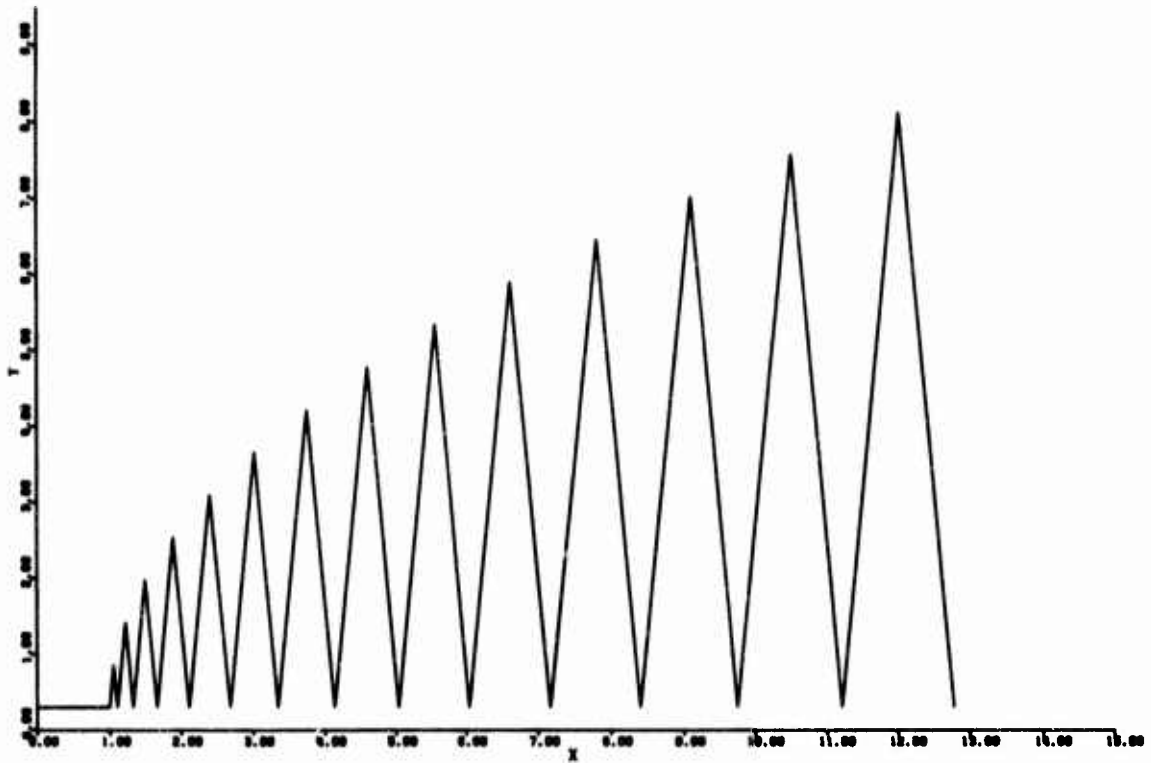


Figure 25. Loading Program.

decreasing load sequence.

Examples of the recorded stress-strain relations for the increasing load sequence are shown in figures 26, 27, and 28 for silty clay, silty sand, and WES loess specimens, respectively. Figure 26a shows the results of applying 46 cycles of increasing load to a specimen of silty clay. These 46 cycles were applied continuously without a rest period. At the end of the 46th cycle there was a short rest period while the recording paper was changed. After the rest period the increasing load sequence was continued and the results of cycles 47 through 67 were recorded in figure 26b. The recording was approaching the top of the paper on cycle 63 necessitating a change in stress scale during this cycle. The scales corresponding to various sections of the recording are shown on the figure. At the end of cycle 67 there was a short rest period as the recording paper was changed. The increasing load sequence was again continued and the results for cycles 68 through 83 are shown in figure 26c. At the end of the 82nd cycle the pen of the recorder was shifted electronically to the left and up because the strain was becoming large with the recording approaching the edge of the paper. The loading curve for cycle 83 is shown above the main recording and as can be seen failure of the specimen occurred on the 83rd cycle. Similar procedures were used for the recordings in figures 27 and 28.

The result of applying the decreasing load sequence shown in the bottom of figure 25 to a specimen of silty sand is shown in the top of figure 29. This same decreasing load sequence was applied to a specimen of silty clay producing the results shown in the bottom of figure 29. However, the specimen of silty

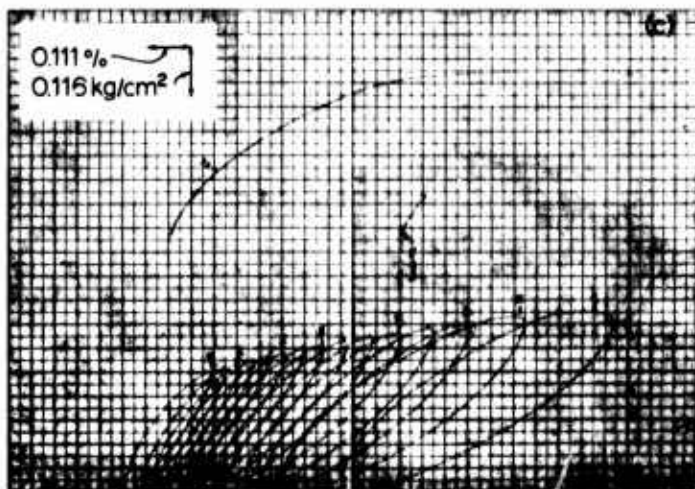
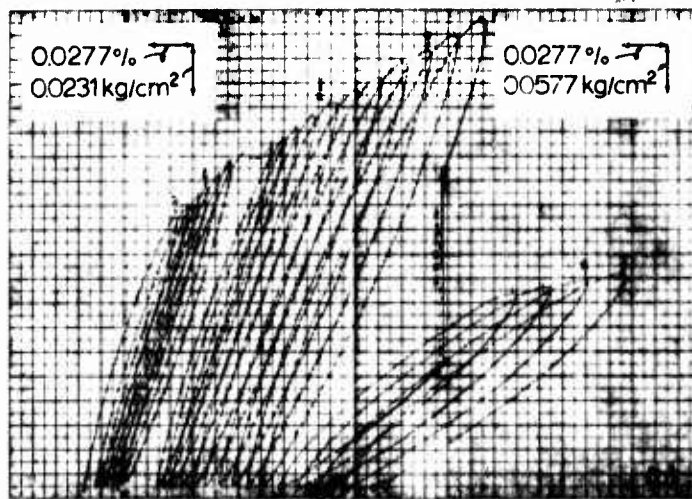
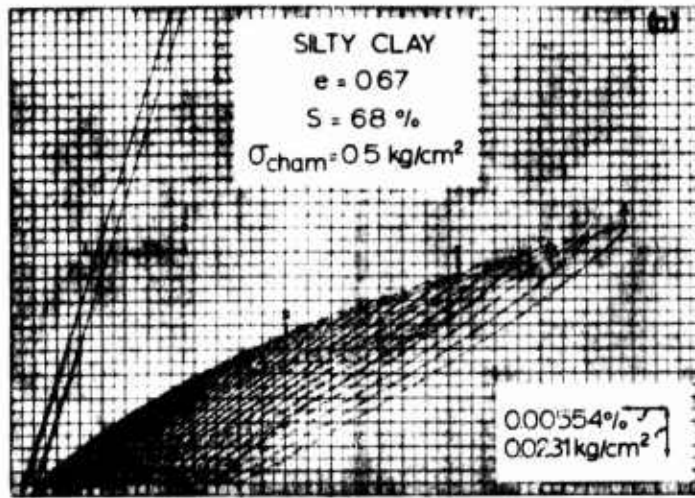


Figure 26. Recorded stress-strain relation, increasing load sequence, silty clay.

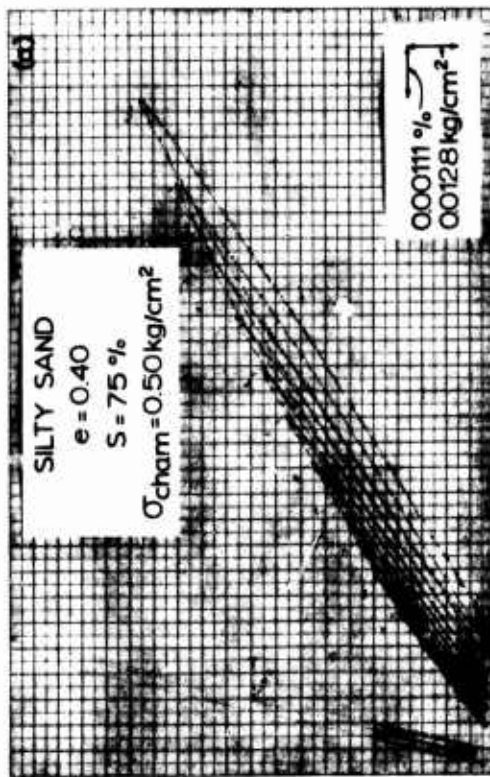
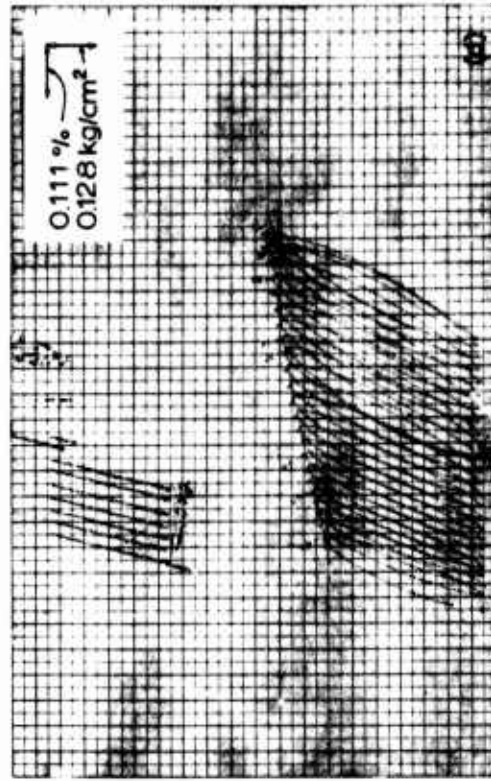
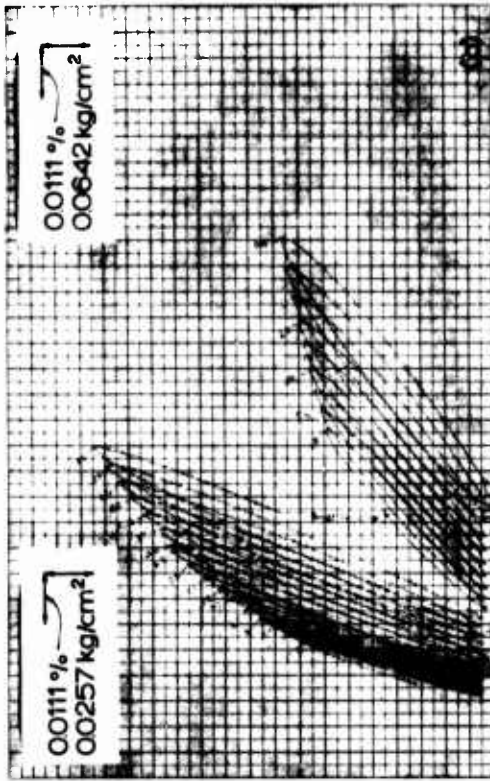


Figure 27. Recorded stress-strain relation, increasing load sequence, silty sand.

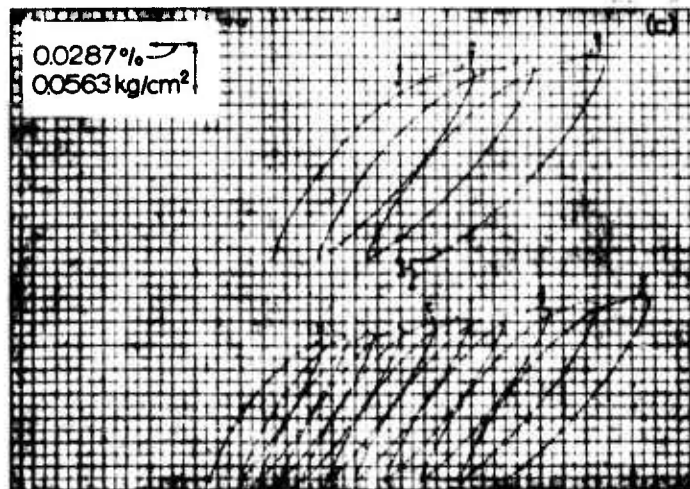
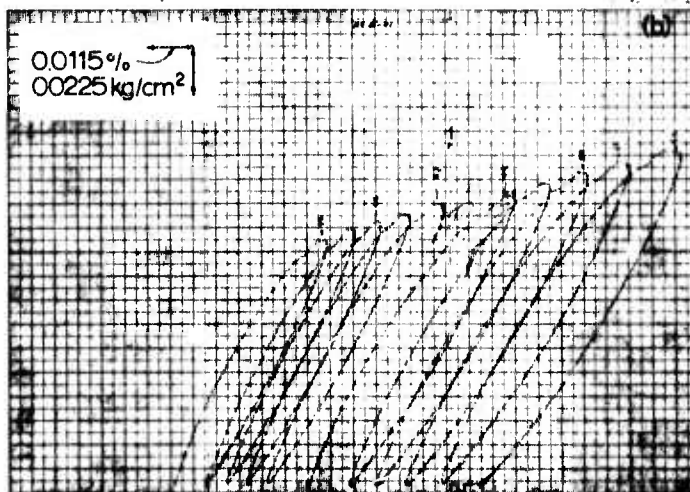
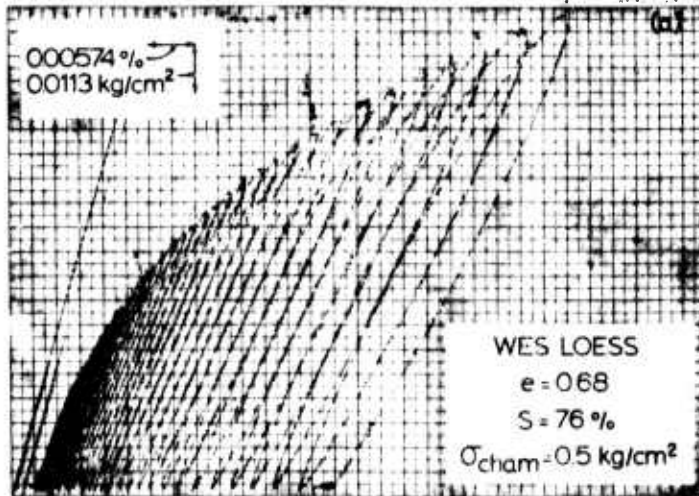


Figure 28. Recorded stress-strain relation, increasing load sequence, Vicksburg Loess.

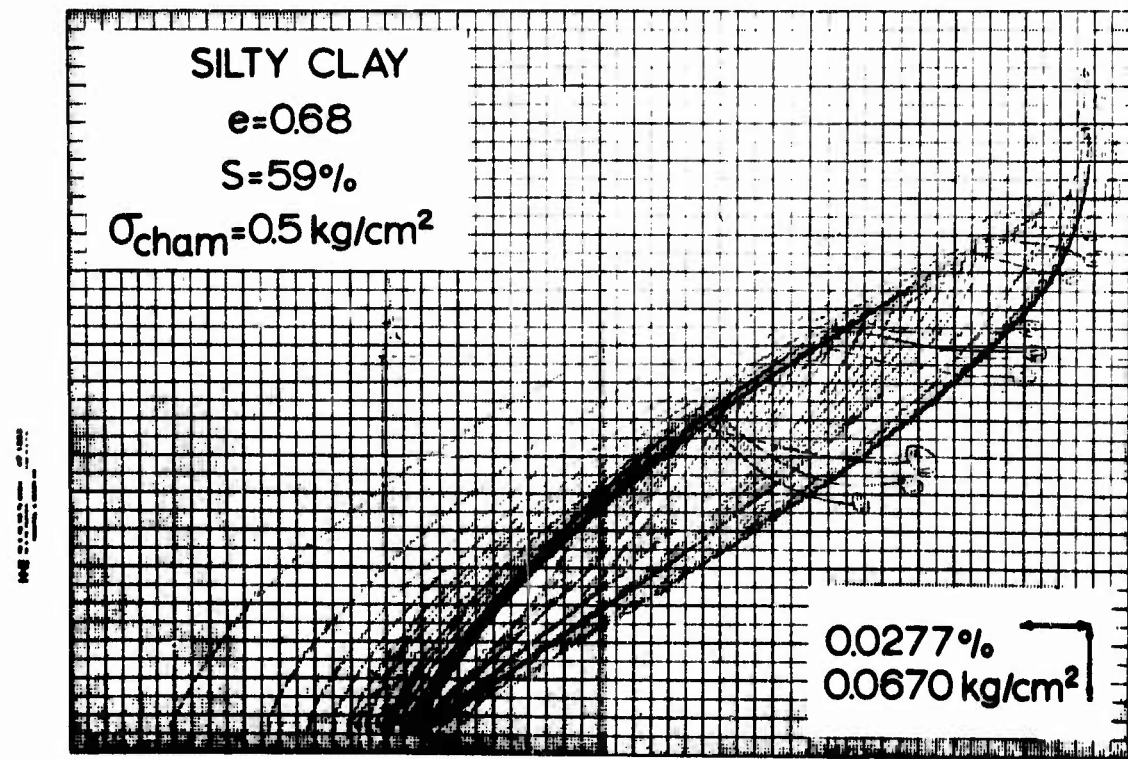
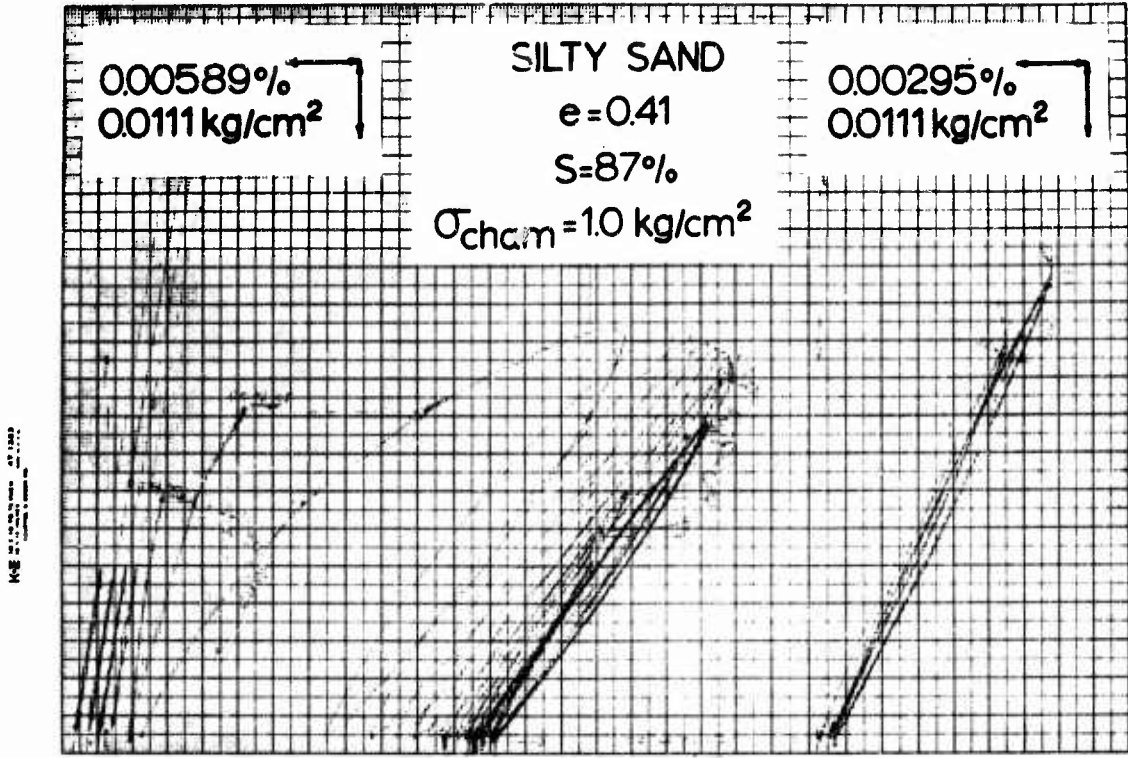


Figure 29. Recorded stress-strain relation, decreasing load sequence.

clay had previously been subjected to the increasing load sequence in the top of figure 25. From these results it can be seen that for decreasing load sequences there is little additional accumulation of set strain as the smaller and smaller loads are applied. Hence, the curves for successive loads trace over the same area of the recording.

### 3. Effect on the Shear Modulus

The values of normalized modulus for all of the mixed amplitude tests are plotted versus normalized strain for the silty clay in figure 30 and for the silty sand in figure 31. The open symbols are for increasing amplitude loading sequences and the solid symbols are for decreasing amplitude loading sequences. Also shown on these figures are the curves calculated from equations 8 and 9 for values of  $a = 0$  and  $a = 2$ . As shown in figure 17, the value of  $a$  for the first cycle of test no. 21 on the Air Force silty clay is 3.50. This value decreased with number of cycles and approaches zero for a large number of cycles. For the first cycle of test no. 4 on the Air Force silty sand in figure 16 the value of  $a = 5.34$ . Again this value approaches zero for a large number of cycles. Since most of the values shown in figures 30 and 31 fall in the range between  $a = 0$  and  $a = 2$ , it appears that the effects of the mixed amplitudes and rest periods on the shear modulus are smaller than the scatter in measured values from test to test of the same soil. Therefore, it is concluded that for practical purposes the procedure outlined in Section II can be applied to mixed traffic conditions.

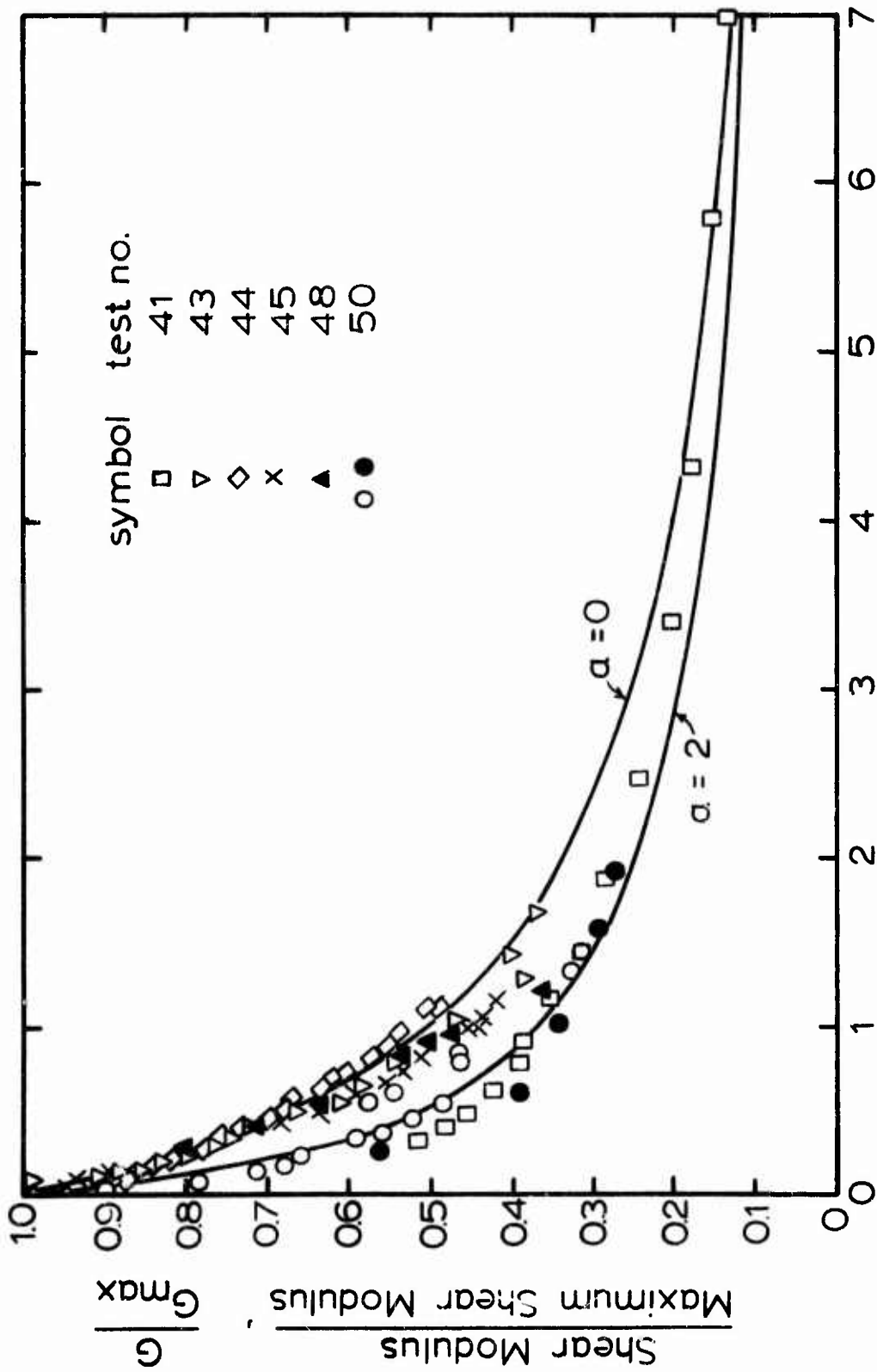


Figure 30. Normalized shear modulus versus normalized strain for silty clay, mixed amplitudes and rest periods.

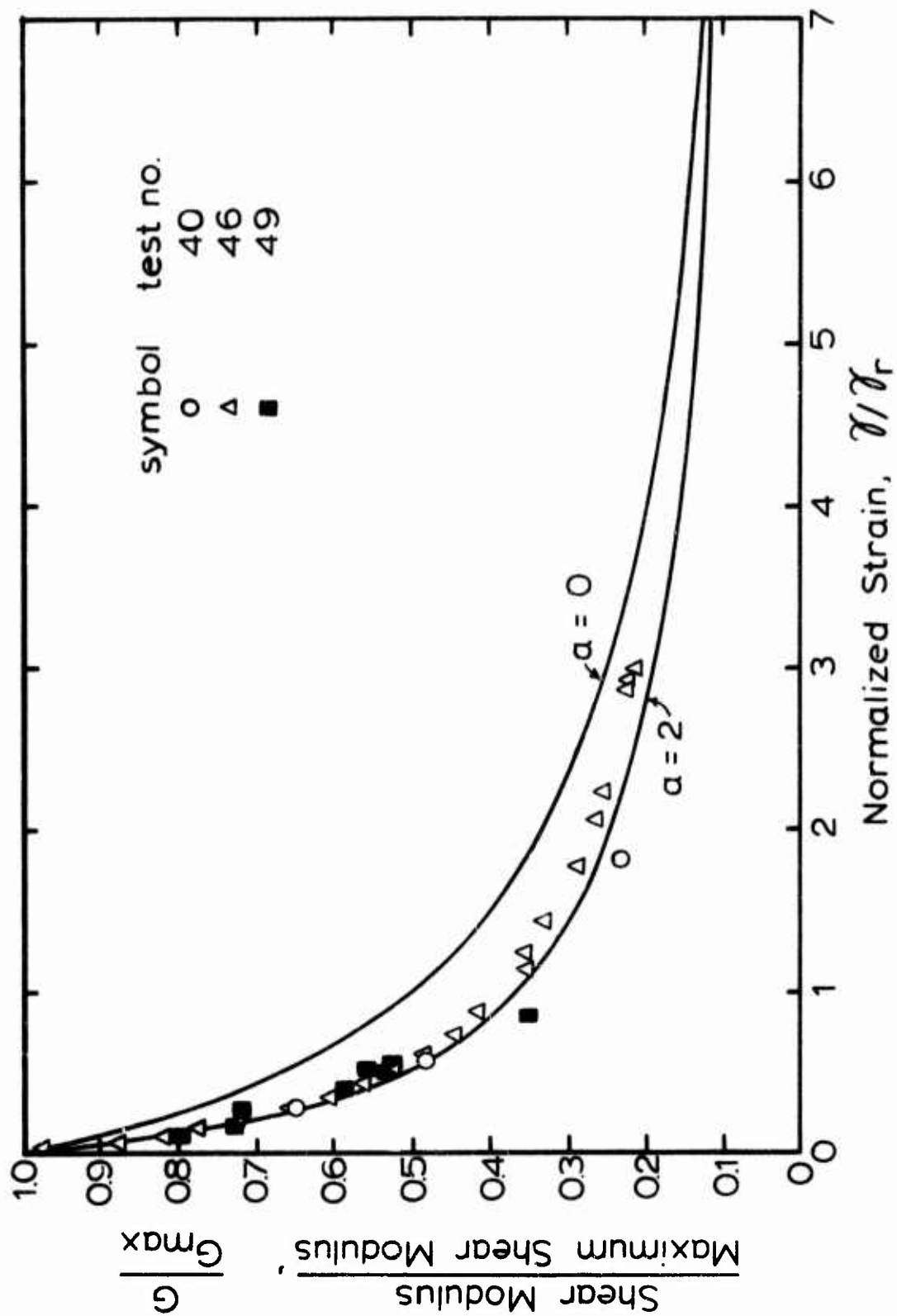


Figure 31. Normalized shear modulus versus normalized strain for silty sand, mixed amplitudes and rest periods.

## SECTION V

### CONCLUSIONS

1. A practical procedure for reducing the shear modulus of soils with increasing strain amplitude has been developed. It has been shown that the procedure gives reasonably accurate results compared to values measured in the laboratory, for a wide variety of soil types and conditions. The study of mixed amplitudes and rest periods indicates that the procedure can also be applied to mixed traffic conditions.

2. The shear modulus of soils in general varies between extreme limits. It may commonly be less than 1000 psi or greater than 50000 psi. Likewise, the relationship between shear modulus and strain level is extremely variable. The picture can be simplified by normalization. The shear modulus is normalized by considering  $G/G_{\max}$ , but the relationship between normalized shear modulus and strain level is still quite variable; because, a given strain does not have the same effect on all soils or on the same soil under different states of stress. When strain is also normalized by dividing by the reference strain,  $\gamma_r = \tau_{\max}/G_{\max}$ , a single relationship for all soils between normalized shear modulus and normalized strain is approached. However, this relationship is still affected somewhat by soil type, percent saturation, and number of cycles and rate of loading. A single relationship for all soils and conditions is finally obtained by defining the hyperbolic strain that depends mainly on the normalized strain but accounts for the residual effects of soil type,  $S$ ,  $N$ , and  $T$ . Hence, these concepts of reference strain and hyperbolic strain have made possible the

development of the practical procedure of paragraph 1.

3. The 123 simple shear tests of 24 different soils reported herein show the following parameter effects on the relationship between normalized shear modulus and normalized strain. For a given value of normalized strain, the normalized shear modulus increased with number of cycles of loading, decreased with increasing percent saturation, and increases with rate of loading. There appears to be very little effect of void ratio on this relationship.

4. The reference strain that is so important to the procedure of paragraph 1 depends on  $\tau_{\max}$  and  $G_{\max}$ . For pavement evaluation the value of  $G_{\max}$  is to be determined by the nondestructive vibratory test. It is not desirable to have to measure the value of  $\tau_{\max}$ . In this study a relationship between reference strain and  $G_{\max}$  has been established, eliminating the necessity for estimating  $\tau_{\max}$ . The relationship depends on void ratio, percent saturation and plasticity index of the soil. It is best defined for nonplastic and low plasticity soils, where the data in figures 13 and 14 indicate that the error is less than 25 percent for about 50 percent of the cases. It should be remembered that a 25 percent error in the value of  $\gamma_r$  does not produce a correspondingly large error in the determination of  $G$ . For a value of normalized strain of one, a 25 percent error in reference strain produces about 12 percent error in the determination of  $G$ . The relationship is much less well defined for high plasticity soils with liquid limit greater than 50, where the error in determination of reference strain may be greater than 100 percent.

5. Assuming the normalized strain is accurately known, the error to be

expected in the relationship between normalized strain and normalized shear modulus is shown by the data in figures 16 through 24, where the vast majority of points fall within plus or minus 20 percent.

6. Finally, an electromagnetic, hollow cylinder, simple shear test capable of accurate measurement of the stress-strain relations for soils over a wide range of strains, from about  $10^{-5}$  in/in to strains corresponding to failure, and where the loading can be programmed to test effects of mixed amplitudes and rest periods has been developed.

## APPENDIX I

### DERIVATION OF REFERENCE STRAIN EQUATION

Neglecting the effects of overconsolidation, for a simple shear state of stress

$$\tau_{\max} = \bar{\sigma}_o \sin \bar{\phi} \quad (12)$$

where  $\bar{\sigma}_o$  = effective mean principal stress and  $\bar{\phi}$  = effective angle of shearing resistance. Also as stated in reference 1,

$$G_{\max} = 1230 F \bar{\sigma}_o^{1/2} \quad (13)$$

Equation 13 is based on many tests of saturated soils. Solving for  $\bar{\sigma}_o$  in equation 13, substituting into equation 12 and replacing the factor 1230 by R, since this factor may not be constant for partially saturated soils

$$\tau_{\max} = \frac{G_{\max}^2 \sin \bar{\phi}}{R^2 F^2} \quad (14)$$

As shown in reference 2, the effective angle of shearing resistance can be defined approximately by

$$\sin \bar{\phi} = 0.6 - 0.25 (PI)^{0.6} \quad (15)$$

Substituting equation 15 into equation 14

$$\tau_{\max} = \frac{G_{\max}^2}{R^2 F^2} [0.6 - 0.25 (PI)^{0.6}] \quad (16)$$

The reference strain

$$\gamma_r = \frac{\tau_{\max}}{G_{\max}} \quad (17)$$

2. Lambe, T. W. and Whitman, R. V., Soil Mechanics, Wiley, 1969, p. 307.

Substituting equation 16 into equation 17

$$\gamma_r = \frac{G_{\max}}{R^2 I^2} [0.6 - 0.25 (PI)^{0.6}] \quad (1)$$

## APPENDIX II

### TESTING METHODS AND PROCEDURES

A simple shear test, where a hollow cylinder of soil was confined in a pressure chamber and loaded torsionally about the axis of the cylinder, was employed for this research. The torsional load was applied electromagnetically by regulating the voltage to four large coils within the fields of four corresponding permanent magnets. The system was capable of applying a maximum torque of approximately 60 kg-cm. The voltage was produced by a wide frequency range, triangular wave signal generator, amplified by a 50 watt DC amplifier. With this electromagnetic system the rate and amplitude of loading could be changed by simply turning the appropriate knob on the signal generator. The rate of loading for the tests varied from approximately 0.2 to 450 kg/cm per hr. Inertial forces were negligible for these rates of loading. Torque and angular motion were measured with electrical transducers located inside the pressure chamber, thus eliminating the influence of friction and apparatus deformation on the measurements. The signals from these transducers were recorded with an X-Y recorder.

Most of the soil specimens tested were subjected to approximately 1000 cycles of a constant-amplitude shear stress. Examples of the recorded shear stress-strain relations are shown in figure 32. This figure illustrates the range of strain amplitudes tested. For test no. 7, top of figure 32, the cyclic shear stress was approximately 80 percent of the strength of the sample. For test no. 15, record no. 1, bottom of figure 32, the cyclic shear stress was only 2.5

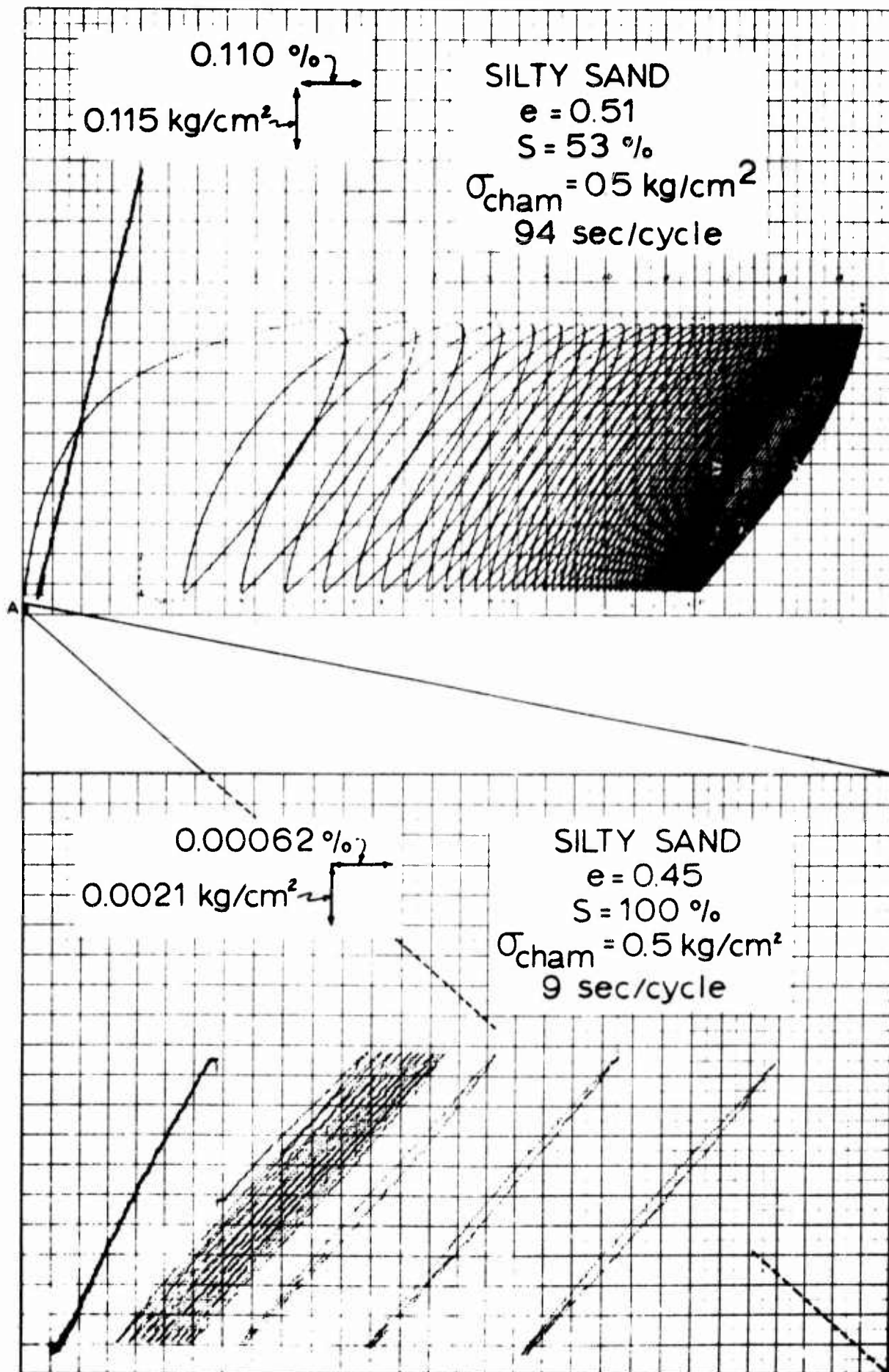


Figure 32. Typical recorded stress-strain relations.

percent of the strength of the sample. The entire graph sheet for test no. 15, if changed to the scale of test no. 7, would fit in the small black rectangle at A in the lower left corner of test no. 7. Cyclic loading tests were conducted for strain amplitudes as small as about  $10^{-5}$  in/in to strain amplitudes as large as  $0.5 \times 10^{-2}$  in/in. After the cyclic loading of each sample, the load was increased to failure in order to measure  $\tau_{\max}$ .